Energy Storage Materials 42 (2021) 129–144

Contents lists available at ScienceDirect

Energy Storage Materials

journal homepage: www.elsevier.com/locate/ensm

# Uncovering electrochemistries of rechargeable magnesium-ion batteries at low and high temperatures

Muhammad Asif, Seamus Kilian, Muhammad Rashad*

*Department of Chemical Sciences, Bernal Institute, University of Limerick, Limerick, V94 T9PX, Ireland*

ARTICLE INFO

*Keywords:*
Magnesium ion batteries
Magnesium-Lithium hybrid ion batteries
Transition metal oxides
Polyanion materials
Nucleophilic/non-nucleophilic electrolytes
High temperature
Ultra-low temperature
Electrochemical properties

ABSTRACT

Rechargeable magnesium ion batteries, which possess the advantages of low cost, high safety, high volumetric capacity, and dendrite free cycling, have emerged as one of the potential contenders alleviate the burden on existing lithium ion battery technologies. Within this context, the electrochemical performance of Mg-ion batteries at high and ultra-low temperatures have attracted research attention due to their suitability for use in extreme environments (i.e. military and space station purposes). To meet the requirements for operation over wide temperature ranges, extensive studies are being conducted to explore different cathodes, anodes, electrolytes, and interfacial phenomena. There is no review that compares the characteristics of magnesium ion batteries in terms of their working mechanism, current challenges, working voltages, possible cathode materials, and resultant electrochemistry at different temperatures. To fulfil this research gap, we summarize the recent advances made in the development of magnesium ion batteries, including high-capacity cathodes, nucleophilic and non-nucleophilic electrolytes, hybrid ion tactics, working mechanisms, their high temperature and ultra-low temperature electrochemical performances. Future recommendations for the development of magnesium ion batteries with high energy densities capable of operating under extreme environmental conditions are also presented.

## 1. Introduction

To mitigate the potential effects of global warming, we need to reduce our reliance on fossil fuels, which (such as coal, oil, gas etc.), that are diminishing rapidly and transition to renewable energy sources (such as wind, sun, water etc.). Li-ion batteries (LIBs) emerged as efficient devices, which can be used in electric vehicles and portable electronics, due to their high energy densities (100-265 Wh/kg) [1]. Despite the commercial success of LIBs and its dominance in the current market, LIB technologies still present specific drawbacks. Critically, Li resources are very limited and diminishing with time due to the ever-increasing demand. In addition, due to the intensive research on LIBs over the past three decades, their electrochemical performance (i.e., specific capacity) is approaching the theoretical limits [2]. There is an urgent need to find alternative energy storage technologies with high energy densities to support LIB technology in matching the ever-increasing demands of energy storage devices across all sectors (EV, mobile and stationary storage) [3–6].

Several post-lithium ion technologies focused on the use of earth-abundant and low cost elements have emerged including those based on sodium [7], potassium [8], aluminum [9], and magnesium [10]. Magnesium as a candidate possesses several advantages compared to lithium. For example, magnesium is about 2.3 wt.% of earth's crust, making it significantly more abundant than lithium [11]. Another attractive feature of Mg-ion batteries is the potential for use of a pure metal anode that could be repackaged or easily recycled as Mg metal allows for dendrite free cycling (unlike Li metal anodes). Magnesium is environmentally friendly owing to its low-toxicity, making it an ideal candidate for eco-friendly energy storage devices [12]. Moreover, Mg is a lightweight metal (1.74 g.cm$^{-3}$ density) [13] yielding a theoretical volumetric capacity of magnesium (3833 mA h cm$^{-3}$) that is twice than that of lithium (2061 mA h cm$^{-3}$) [14]. Similarly, the reduction potential of magnesium is also higher than that of lithium i.e. -2.36 V (for Mg) and -3.04 V (for Li) vs. $H^+/H_2$ [15]. A comparison illustrating the different chemical properties of magnesium and lithium is shown in Table 1.

Due to the attractive properties of magnesium described above, considerable research attention has been given into developing new kinds of organic and inorganic electrolytes, high voltage cathodes, and to understand the electrochemical mechanism of magnesiation and demagnisiation. Apart from academic researchers, industries such as Pellion Technologies, Toyota Research Institute of North America, and Sony Corporation have started research and development projects for rechargeable magnesium batteries. The emphasis of these R & D projects is on the overcoming the challenges associated with the practical application of magnesium batteries at an industrial scale [16,17]. To date, improving the cycling and rate performance of magnesium batteries has proven

* Corresponding author.
*E-mail address:* Muhammad.Rashad@ul.ie (M. Rashad).

https://doi.org/10.1016/j.ensm.2021.07.031
Received 11 June 2021; Received in revised form 15 July 2021; Accepted 21 July 2021
Available online 25 July 2021

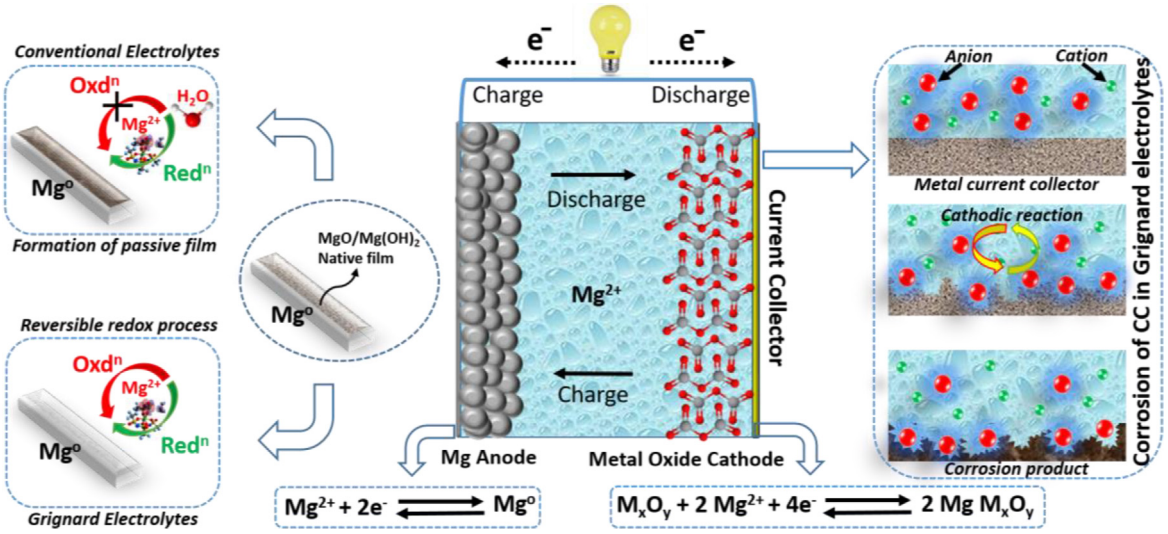


**Fig. 1.** Schematic illustration of rechargeable Mg batteries with redox reactions occurring at both anode and cathode sides, and highlights of recent challenges.

**Table 1**
Key parameter comparisons between magnesium and lithium metals for rechargeable metal ion batteries [10].

| Information | Lithium | Magnesium |
|---|---|---|
| Market price (k$/ton) | 64.8 | 2.7 |
| Volumetric capacity (mAh $cm^{-3}$) | 2061 | 3833 |
| Gravimetric capacity (mAh $g^{-1}$) | 3884 | 2206 |
| Anode potential versus SHE [V] | –3.04 | –2.36 |
| Stability in air? | No | Yes |
| Dendrite growth? | Yes | No |
| Atomic weight | 6.9 | 24.3 |
| Cationic radius (nm) | 0.068 | 0.065 |

difficult owing to the lack of high potential cathodes and electrolytes that can accommodate and transport the magnesium ion [18].

Generally, magnesium batteries consist of a cathode, anode, electrolyte, and current collector. The working principle of magnesium ion batteries is similar to that of lithium ion batteries and is depicted in Fig. 1 [13]. The anode is made of pure magnesium metal or its alloys, where oxidation and reduction of magnesium occurs with the help of magnesium ions present in the electrolyte (e.g., PhMgCl-$AlCl_3$/THF solution) [19]. Cathode materials require good chemical stability and high capability to reversibly intercalate/deintercalate magnesium ions during redox reactions. The desired characteristics of cathodes are low cost, high magnesium ion reversibility, and adequate operating voltage. Normally, the cathode consists of a transition metal oxide, where insertion or extraction of magnesium ions take place during the discharge/charge process, respectively, (Table 2).

## 2. Current challenges

As discussed above, the magnesium metal anode is an important component of magnesium battery, thus it is essential to choose an electrolyte compatible with the anode to obtain good cycle life and coulombic efficiency. Like lithium technology, the presence of moisture or carbonates/perchlorate based salts in electrolytes adversely affect the magnesiation/demagnisiation process on magnesium anode. Reports suggest that these will passivate the surface of the anode (formation of non-permeable solid-electrolyte interphase), causing the battery to exhibit poor coulombic efficiencies and cycle life [20]. Thus, only Grignard based electrolytes such as tetrahydrofuran (THF) based magnesium organochloroaluminate electrolyte complex have demonstrated compatibility with magnesium metal anodes to date. These electrolyte lead to the formation of solid-electrolyte interphase layer on the anodes surface, facilitating improved performance [21]. The challenges associated with the electrolyte/anode compatibility have triggered the development of organic and inorganic electrolyte complexes that prohibit surface passivation of the magnesium anodes [13]. Besides the passivation issues, another problem associated with magnesium metal is its anodic stability. The available electrolytes based on ethyl-magnesium bromide and butyl-magnesium chloride, exhibit anodic stabilities of about 1.3 V vs. Mg, which is not sufficient for the commercialization of magnesium batteries. This results in less choice to select suitable and stable anode materials. Several attempts were made to attain better anodic stabilities by employing different electrolytes such as $Mg(AlH_4)_2$, $MgBr_2$, $Mg(BH_4)_2$, $Mg(B(C_4H_9)_4)_2$, and $Mg(AlCl_2BuEt)_2$ based electrolytes [22–24].

The stability of current collectors is also an important aspect for designing a rechargeable magnesium battery. Studies have shown that both current collector and electrolyte must be compatible to prevent side reactions. It was observed that magnesium organohaloaluminates containing magnesium dimer cation $(Mg_2(\mu\text{-}Cl)_3\bullet 6THF)^+$ are highly corrosive in nature. Therefore, common metal current collectors such as Al, Ni, Cu, and SS exhibit poor stabilities in these electrolyte solutions [25]. Thus, the above mentioned electrolytes require free standing cathodes or special current collectors such as graphite or carbon paper. To resolve this issue, several recent studies were conducted involving extensive characterization to attain mechanistic insights into chlorine free electrolyte complexes that are non-corrosive in nature [26-28].

Another major obstacle in the development of magnesium batteries is the availability of non-corrosive electrolytes capable of transporting magnesium ions during redox reactions. As mentioned above, carbonate-based electrolytes are not suitable for magnesium stripping and plating process. The main reason for this is the formation of a passivation layer on magnesium anode surface, which is due to the chemical reduction of solvents and anions present in these electrolytes [20,29,30]. The first breakthrough reported the capability of Grignard solutions to reversibly strip and deposit magnesium. This finding has triggered the research on exploring more efficient and stable electrolytes by modifying the Lewis acid-base reactions occurring between aluminum and magnesium reagents [30-33]. Despite the impressive reversibility, use of Grignard solution based electrolytes is restricted owing to their nucleophilic characteristics, preventing the use of high capacity electrophilic cathodes (such as sulfur). This non-compatibility of magnesium organo-haloaluminate electrolytes has inspired researchers to focus on the development of non-nucleophilic magnesium electrolytes [10,34–36]. Several successful attempts were made to synthesize new non-

**Table 2**
Summary of low and high temperature electrochemical properties of magnesium ion batteries.

| Materials | Electrolytes | Potential Window (V) | Capacity/Current Density($mAhg^{-1}$)/($Ag^{-1}$) | Temperatures | References |
|---|---|---|---|---|---|
| $MgIn_2S_4$ | $[Mg(G4)][TFSI]_2$ -[MPPyr][TFSI]-G4 | 1.2 – 3.2 | 500/0.02 | 150 °C | [81] |
| $MgIn_2S_4$ | $[Mg(G4)][TFSI]_2$ -[MPPyr][TFSI]-G4 | 1.2 – 3.2 | 450/0.02 | 100 °C | [81] |
| $MgIn_2S_4$ | $[Mg(G4)][TFSI]_2$ -[MPPyr][TFSI]-G4 | 1.2 – 3.2 | 340/0.02 | 70 °C | [81] |
| $V_2O_5.H_2O$@rGO | $Mg(TFSI)_2$)-AN | 1.5 - 3.4 | 225/1.0 | 55 °C | [75] |
| $VO_2$ | APC-LiCl-THF | 0.5 – 2.0 | 220/0.1 | 55 °C | [77] |
| $MgIn_2S_4$ | $[Mg(G4)][TFSI]_2$ -[MPPyr][TFSI]-G4 | 1.2 – 3.2 | 235/0.02 | 50 °C | [81] |
| $V_2O_5.H_2O$@rGO | $Mg(TFSI)_2$)-AN | 1.5 - 3.4 | 152/1.0 | 40 °C | [75] |
| $VO_2$ | APC-LiCl-THF | 0.5 – 2.0 | 190/0.1 | 40 °C | [77] |
| $VO_2$ | APC-LiCl-THF | 0.5 – 2.0 | 175/0.1 | 30 °C | [77] |
| $Li_3V_2(PO_4)_3$ | $Mg(BH_4)_2$ -$LiBH_4$-DG | 0.0 – 1.5 | 78/0.1 | 25 °C | [91] |
| $Li_3V_2(PO_4)_3$ | APC-LiCl-THF | 0.0 – 2.0 | 135/0.1 | 25 °C | [91] |
| $Li_4Ti_5O_{12}$ | APC-LiCl-THF | 0.0 – 2.0 | 213/0.1 | 25 °C | [99] |
| $V_2O_5.H_2O$@rGO | $Mg(TFSI)_2$)-AN | 1.5 - 3.4 | 115/1.0 | 20 °C | [75] |
| $VO_2$ | APC-LiCl-THF | 0.5 – 2.0 | 150/0.1 | 20 °C | [77] |
| $VO_2$ | APC-LiCl-THF | 0.5 – 2.0 | 90/0.1 | 10 °C | [77] |
| $Li_4Ti_5O_{12}$ | APC-LiCl-THF | 0.0 – 2.0 | 165/0.1 | 10 °C | [99] |
| $V_2O_5.H_2O$@rGO | $Mg(TFSI)_2$)-AN | 1.5 - 3.4 | 75/1.0 | 0 °C | [75] |
| $VO_2$ | APC-LiCl-THF | 0.5 – 2.0 | 35/0.1 | 0 °C | [77] |
| $LiFePO_4$ | APC-LiCl-THF | 2.0 – 2.8 | 103/0.3C | 0 °C | [90] |
| $Li_3V_2(PO_4)_3$ | $Mg(BH_4)_2$ -$LiBH_4$-DG | 0.0 – 1.5 | 69/0.1 | 0 °C | [91] |
| $Li_3V_2(PO_4)_3$ | APC-LiCl-THF | 0.0 – 2.0 | 117/0.1 | 0 °C | [91] |
| $Li_4Ti_5O_{12}$ | APC-LiCl-THF | 0.0 – 2.0 | 143/0.1 | 0 °C | [99] |
| $LiFePO_4$ | APC-LiCl-THF | 2.0 – 2.8 | 97/0.3C | – 10 °C | [90] |
| $Li_3V_2(PO_4)_3$ | $Mg(BH_4)_2$ -$LiBH_4$-DG | 0.0 – 1.5 | 55/0.1 | – 10 °C | [91] |
| $Li_3V_2(PO_4)_3$ | APC-LiCl-THF | 0.0 – 2.0 | 103/0.1 | – 10 °C | [91] |
| $Li_4Ti_5O_{12}$ | APC-LiCl-THF | 0.0 – 2.0 | 133/0.1 | – 10 °C | [99] |
| $V_2O_5.H_2O$@rGO | $Mg(TFSI)_2$)-AN | 1.5 - 3.4 | 65/1.0 | – 15 °C | [75] |
| $LiFePO_4$ | APC-LiCl-THF | 2.0 – 2.8 | 90/0.3C | – 20 °C | [90] |
| $Li_3V_2(PO_4)_3$ | $Mg(BH_4)_2$ -$LiBH_4$-DG | 0.0 – 1.5 | 35/0.1 | – 20 °C | [91] |
| $Li_3V_2(PO_4)_3$ | APC-LiCl-THF | 0.0 – 2.0 | 93/0.1 | – 20 °C | [91] |
| $Li_4Ti_5O_{12}$ | APC-LiCl-THF | 0.0 – 2.0 | 78/0.1 | – 20 °C | [99] |
| $V_2O_5.H_2O$@rGO | $Mg(TFSI)_2$)-AN | 1.5 - 3.4 | 40/1.0 | – 30 °C | [75] |
| $Li_3V_2(PO_4)_3$ | APC-LiCl-THF | 0.0 – 2.0 | 82/0.1 | – 30 °C | [91] |
| $LiFePO_4$ | APC-LiCl-THF | 2.0 – 2.8 | 80/0.3C | – 40 °C | [90] |
| $Li_3V_2(PO_4)_3$ | APC-LiCl-THF | 0.0 – 2.0 | 63/0.1 | – 40 °C | [91] |

nucleophilic magnesium ion electrolytes that exhibit good ionic conductivities, oxidation stabilities, and fast magnesium plating/stripping. The well-known magnesium organohaloaluminate electrolytes include di-chloro complex (DCC) electrolytes, and the all-phenyl complex (APC), etc. that have been analyzed in previous reports [10,13]. Among the new developments, the best non-nucleophilic magnesium ion electrolytes in terms of their compatibility with electrophilic cathodes, are hexamethyldisilazide (HMDS)-based electrolytes, magnesium aluminum chloride complex (MACC) electrolytes, $Mg(TFSI)_2$-based electrolytes, and boron-containing Mg-ion electrolytes [37].

In terms of cathode development for MBs, the initial breakthrough was made by Aurbach et al. [38] in 2000, where Chevrel phases were explored as host materials for magnesium ion intercalation. This prototype magnesium ion battery exhibited moderate energy density (60 W h $kg^{-1}$) and operating voltage (1.2 V vs. $Mg/Mg^{2+}$) and triggered research on post-Chevrel phase cathodes. These include the discoveries of high voltage intercalation type cathode materials such as transition metal oxides, metal sulfides, and polyanion type materials etc., and high capacity conversion type cathode materials such as selenium, sulfur, copper sulfides, carbon florins, bromine, and iodine [39-41]. The conversion type cathodes may exhibit high capacities because magnesium ions are stored via bond formation/deformation process with the active material (e.g., sulfur). The advantage of such cathode materials is that it does not involve sluggish solid-state diffusion of magnesium ions into solid lattices. However, the deformation of bonds in magnesium-conversion cathode materials might be difficult and thus, the choice of electrolyte is a crucial factor. Majority of the conversion type cathodes result in the formation of intermediate products that are soluble in the electrolytes [42-45]. On the other hand, a major drawback of high voltage (2 – 3 V) intercalation type cathodes is the irreversible trapping of magnesium ions inside the host material due to strong electrostatic interactions. The Mg ion trapping in the host material results in rapid capacity fade. Thus, despite their high voltage characteristics, these cathodes are not ideal candidates for practical applications.

## 3. Migration barriers

Another obstacle to the advancement of magnesium ion batteries (MIBs) is sluggish transportation of $Mg^{2+}$ ions (caused by migration barrier) inside the solid materials [46]. Unlike, sodium or lithium ion batteries, the poor mobility of $Mg^{2+}$ ions and other divalent or trivalent cations restricts the development of broad range of host materials for next generation rechargeable metal ion batteries [47]. As a result, the slow magnesium transportation will restrict the utilization of solid barrier coatings to protect the electrodes from side reactions with liquid electrolytes, which will ultimately limits the development of full cell MIBs. Literature studies revealed that several pioneering theoretical and experimental works were successfully conducted to develop the semi and fully solid state, multivalent, and high temperature conductors, which exhibited sufficient conductivities (i.e. ($\sim 3 \times 10^{-2}$ mS $cm^{-1}$) at temperatures ranging from 400 to 800 °C [48,49]. However, the high RT conductivities remained indefinable due to slow migration of $Mg^{2+}$ ions. Recently, P. Canepa et al. [50] proved that $Mg^{2+}$ ion mobility could be enhanced in solid host materials via judicious tuning of crystal structure and chemistry. They mechanistically investigated the room temperature conduction of $Mg^{2+}$ ion by combining ***ab*** anitio calculations, synchrotron X-ray diffraction, electrochemical impedance spectroscopy, and solid-state nuclear magnetic resonance (SS-NMR). First generation of crystalline solids including spinal $MgX_2Z_4$, with X = (In, Y, Sc) and Z = (S, Se), was discovered, and it possess high $Mg^{2+}$ cation mobility at room temperature. Furthermore, the practical design rules to identify fast multivalent-ion solid conductors were proposed, where theoretical

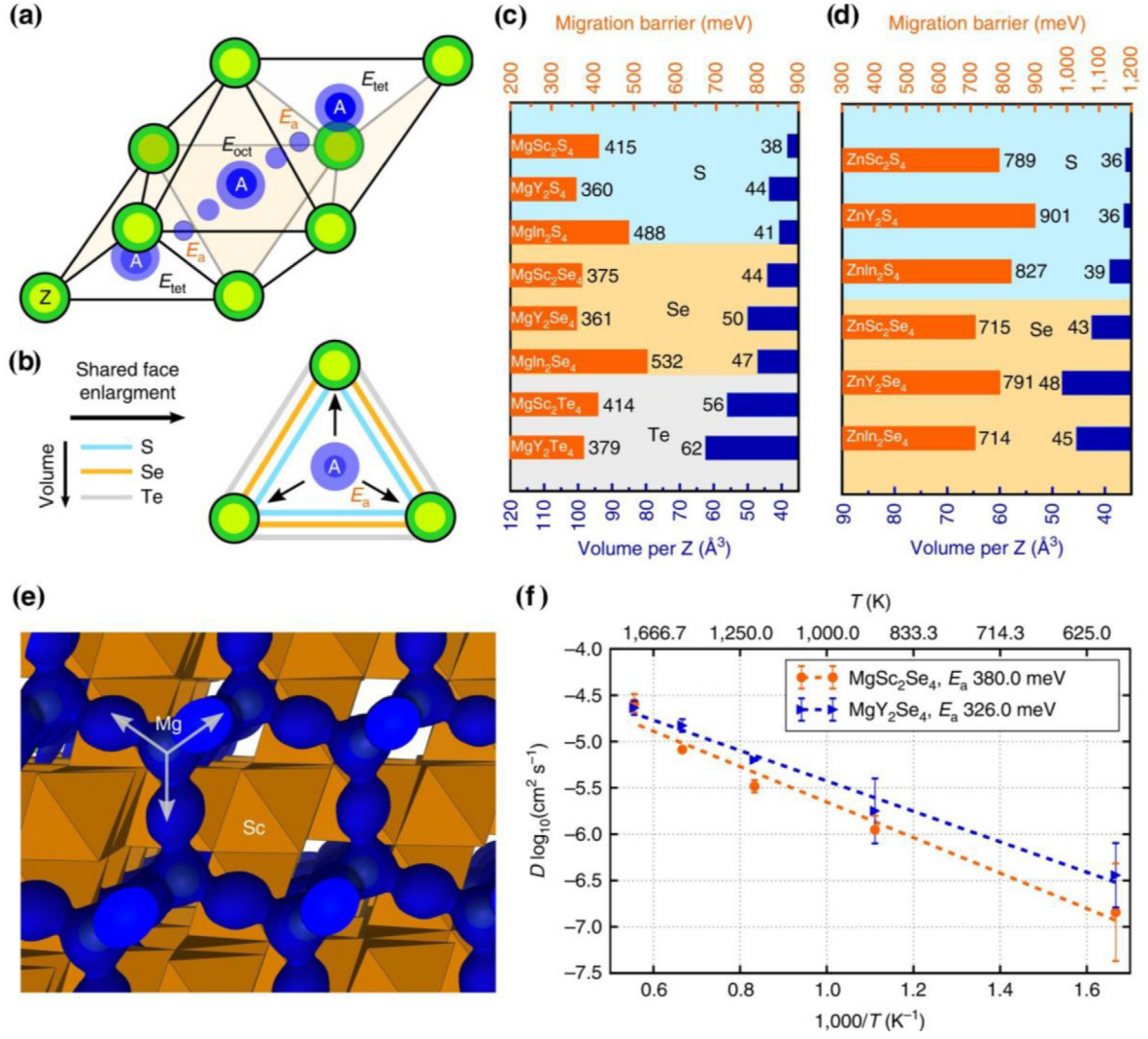


**Fig. 2.** First-principles Mg and Zn migration barriers in sulfides, selenides, and tellurides $AX_2Z_4$ spinels (with A = Mg or Zn). (a) tet-oct-tet migration path in the $AX_2Z_4$ framework, with energy of the tet, oct, and transition sites indicated by $E_{tet}$, $E_{oct}$, $E_a$, respectively. $E_a$ corresponds to the migration energy. (b) Effect of the anion size on the shared (triangular) face between tet and oct sites. (c) and (d) computed Mg and Zn migration barriers (orange bars in meV) in $AX_2Z_4$ spinel and volume per anion (blue bars), respectively, with X = Sc, Y, and In, and Z = S, Se and Te. (e) Mg probability density in $MgSc_2Se_4$ at 900 K obtained from ab initio molecular dynamic simulations (AIMDs). (f) Mg diffusivities as extrapolated from AIMD in $MgSc_2Se_4$ (orange) and $MgY_2Se_4$ (blue), with dashed lines and error bars indicating Arrhenius fits and SD, respectively (Reproduced with permission from [50] Copyright Nature (2017)).

calculations and electrochemical experiments recommended that sulfide and selenide spinels could potentially integrate with current state-of-the-art Mg cathodes, e.g., spinel-$MgTi_2S_4$ and Chevrel-$Mo_6S_8$ [38,51].

As shown in Fig. 2 [50], it was found that the ion migration between two tetrahedral sites (tet) take place via a vacant octahedral site (oct) in spinel structures. Where face-shares with the tetrahedral sites, followed by the migration topology tet-oct-tet of Fig. 2a-b. The energy of the migrating ion in the shared triangular face between oct and tet sites ($E_a$, of Fig. 2b) determine the magnitude of migration barrier. As a result, value of $E_a$ is affected by the size of triangular face and its constituent species. The migration barriers for Mg and Zn (represented by orange bars) were calculated using first principles (DFT)-based nudged elastic band calculations in spinel $AX_2Z_4$ structures (with A = Mg or Zn, X = Sc, Y and In, and Z = S, Se and Te) as shown in Fig. 2c-d [52]. Furthermore, Fig. 2e-f represents the magnesium probability density in $MgSc_2Se_4$ and the trend of diffusivities as a function of temperature in $MgSc_2Se_4$ and $MgY_2Se_4$, respectively. All these results (i.e. probability density and diffusivities) were deduced from ab initio molecular dynamic simulations [50].

## 4. Solid-state electrolytes

Like cathode material, electrolyte is also a key component of magnesium ion batteries. The usage of conventional liquid electrolytes is highly dependent on compatibility of electrolyte's constituents with host cathode material and magnesium metal anode. To avoid these challenges, solid-state magnesium ion electrolytes were also studied in past decades. Unlike conventional liquid electrolytes, the diffusion of active ions inside solid-state electrolyte compensate the charge. An ideal solid-state electrolyte should have negligible electronic conductivity, single mobile ion species, wider potential window, high transference number, high thermal and chemical stabilities, compatibility with cathodes and anodes, high ionic conductivity ($10^{-3}$ S/cm), and environmental friendly. During past decades, several attempts were made to explore the solid-state magnesium ion electrolytes including polymers.

First pioneering work on solid-state electrolyte was carried out by Ikeda et al. [48], who studied the conductivity of $Mg^{2+}$ ions in Mg-Zr-$PO_4$. Experimental results revealed that $Mg_{0.5}Zr_2(PO_4)_3$ revealed the ionic conductivities of about $2.9 \times 10^{-5}$ and $6.1 \times 10^{-3}$ S/cm at

400 and 800°C, respectively. The activation conduction energy was found to be 0.82 eV. The Tubandt's technique and electron probe microanalysis were used to confirm that charge carriers were $Mg^{2+}$ ions in this material [48]. Later on, sol-gel method was also adopted to synthesize $Mg_{0.5}Zr_2(PO_4)_3$, which revealed higher ionic conductivity ($6.1 \times 10^{-3}$ S/cm) at the temperature of 725°C with same activation energy [53]. On the other hand, composite electrolyte, which comprises of $ZrO(PO_4)_2$ and $Mg_{0.5}Zr_2(PO_4)_3$ ceramics, exhibited the ionic conductivity of $6.92 \times 10^{-3}$ S/cm at 800°C [54]. The reason for improved conductivity was reduced grain-boundary resistance towards ionic migration, which was attributed to the presence of secondary phase. The net activation energy of above composite was about 1.14 eV, which led to high room temperature conductivities. An important aspect of $Mg_{0.5}Zr_2(PO_4)_3$ system is that Zr- and P-sites can be substituted to accommodate more $Mg^{2+}$ ions in the system. For example, common dopants such as $Si^{4+}$, $Ce^{4+}$, $Nb^{4+}$, $Zn^{2+}$, $Al^{3+}$, and $Fe^{3+}$, can be substituted in the $Mg_{0.5}Zr_2(PO_4)_3$ system [55].

Practically, $Zr^{4+}$ was substituted by $Si^{4+}$ to make $Mg_{0.5}Si_2(PO_4)_3$ system, which exhibited monoclinic structure similar to that of $Mg_{0.5}Zr_2(PO_4)_3$ system [56]. This new system exhibited the ionic conductivity of about $1.06 \times 10^{-6}$ S/cm at room temperature. This value is higher than that of $Mg_{0.5}Zr_2(PO_4)_3$ system. The increased ionic conductivity was attributed to the reduction of unit cell volume, which facilitates the propagation of $Mg^{2+}$ ion in the system. The $Mg_{0.5}Si_2(PO_4)_3$ system revealed the potential window of about 3.2 V, which is much higher than that of inorganic-oxide based electrolytes. However, the activation energy was not estimated in this system. To further, enhance the capability of $Mg_{0.5}Si_2(PO_4)_3$ system, Halim et al. [57] introduced $Al^{3+}$ ions, which helps to create more interstitial sites in the lattice. The final synthesized $Mg_{0.625}Si_{1.75}Al_{0.25}(PO_4)_3$ system revealed the bulk ionic conductivity of about $2.78 \times 10^{-5}$ S/cm at room temperature. This value is higher than ten times the original parent composition. The drawback of $Mg_{0.625}Si_{1.75}Al_{0.25}(PO_4)_3$ system was reduced electrochemical stability window (2.5 V) owing to aluminum doping. Besides NASICON-type solid state magnesium electrolytes, the $\beta$-$MgSO_4$:$Mg(NO_3)_2$-0.4MgO composite was also synthesized using sol-gel method [58]. Synthesized composites exhibited the ionic conductivity of about $2 \times 10^{-6}$ S/cm at room temperature. The high conductivity of composite was attributed to presence of $\beta$-$MgSO_4$ amorphous state in MgO particles. In another work, trivalent-ion-conducting $Sc_2(WO_4)_3$ was used to prepare $Mg[Hf(WO_4)_3]$ with exhibited the ionic conductivity of about $2.5 \times 10^{-4}$ S/cm at the temperature of 600°C with 0.84 eV activation energy [59].

Several attempts were also made to use borohydride-based solid-state magnesium electrolytes. For example, *ab initio* calculations was employed to examine the high temperature propagation of magnesium ions in magnesium borohydrides ($Mg(BH_4)_2$) [60,61]. It was found that $[BH_4]^-$ ions having $Mg^{2+}$ ions in its tetrahedral cages had limited mobility, owing to strong coulombic interactions with $[BH_4]^-$. However, the cage size can be increased by substituting $[BH_4]^-$ ions with $[AlH_4]^-$, making $Mg^{2+}$ ion migrations possible. Inspired from these studies, Higashi et al. [49] found that $Mg^{2+}$ ions in magnesium borohydrides and $Mg(BH_4)(NH_2)$ revealed an ionic-bonding behavior, which was determined from presence of large cavities (facilitating the hopping of $Mg^{2+}$ ion) and Bader charge on the ion. Higashi et al. [49] used DFT data and examined the conductivity of $Mg^{2+}$ ions in these solid materials. Fig. 3a shows the crystal structure of $Mg(BH_4)(NH_2)$, and we can see that replacements of two of four $BH_4$ units with two amine group. This will leads to formation of a tetrahedral cage of $B_2N_2$ around the magnesium ion. The final structure comprise of alternate pilling of $Mg^{2+}$ cations and $BH_4$, $NH_2$ anions along the c-axis. The nearest Mg-Mg ions are arranged in a zigzag fashion with a distance of about 3.59 Å in a-c plane. Authors found the ionic conductivity of about $1 \times 10^{-6}$ S/cm for $Mg(BH_4)(NH_2)$ at 150°C. This ionic conductivity was higher than that of $Mg(BH_4)_2$ measured at same temperatures. The increased ionic conductivity was due to shorter Mg-Mg interatomic distance (3.59 Å), much lesser than that in $Mg(BH_4)_2$ (4.32 Å) and pronounced ionic nature of bonds in $Mg(BH_4)(NH_2)$. Apart from higher ionic conduction, the $Mg(BH_4)(NH_2)$ solid electrolyte showed reversible plating and stripping of $Mg^{2+}$ ion on platinum electrodes as shown in Fig. 3b. In addition, it was noticed that $Mg(BH_4)(NH_2)$ exhibited the oxidative stability of about 3.0 V (against $Mg/Mg^{2+}$) at 150°C. This oxidative stability is higher than that of $Mg(BH_4)_2$-ether based electrolytes at room temperature [62]. Thus, $Mg(BH_4)(NH_2)$ solid electrolyte is suitable for magnesium battery applications above 150°C.

## 5. Research gap

There are several reviews on magnesium ion technology in terms of working mechanism, current challenges and development of anodes, cathodes, and electrolytes. Another report reviewed the progress on non-aqueous multivalent secondary batteries with a focus on magnesium, calcium, and aluminum ion batteries [39]. Huie et al. [46] also discussed positive electrode materials for magnesium batteries. Muldoon et al. [42] highlighted the foremost research in the development of electrolytes and cathodes and discussed some of the significant challenges of magnesium batteries. Zhang et al. [37] summarized the recent advances and future challenges of high-capacity conversion-type cathodes for rechargeable magnesium batteries and proposed guidelines to provide new insights for developing high-energy-density magnesium batteries. Recently, Guo et al. [63] reviewed the advances in the anode materials (metals and their alloys, metal oxides, and two-dimensional materials) available for magnesium batteries and the corresponding Mg-storage mechanisms. Rashad et al. [10,13,64,65] reviewed the various aspects of magnesium ion battery development including the working mechanism, challenges, in situ and interfacial studies, intercalation and conversion type electrodes, magnesium-sulfur and magnesium-selenium technology, and hybrid ion batteries (magnesium-lithium, magnesium-sodium, and magnesium-zinc hybrid technologies).

M. Mao et al. [66] and his coworkers have tried to summarized the challenges faced by Mg-ion batteries by critically reviewing the impact of compositions and structures of cathode materials on magnesiation kinetics. The most representative research articles on conversion materials, water co-intercalation cathodes, Chevrel phase, spinel structure, polyanion, phosphate, and silicate-based cathodes were critically discussed in terms of their electrochemical performance and structural stabilities. Their work provided comprehensive knowledge of magnesium cathodes and strategies for discovering new cathodes for rechargeable magnesium ion batteries, but it was limited to developments made during half decade (till 2018). Later on, Y. Zhang et al. [67] made another attempt to accumulate the advances made in electrode materials developments (including metal sulfides, metal oxides, spinal, Olivine, and NASICON-based electrodes) for pure and hybrid ion batteries.

*One important aspect of Mg-ion batteries that has not been reviewed is their high and low temperature electrochemical performance, despite growing reports on these topics. Thus, this review focusses on wide temperature range magnesium ion batteries including their advantages, drawbacks, low/high temperature electrolyte compatibility, and positive and negative electrode materials.*

## 6. High temperature electrochemistries

Despite the commercial success of LIBs, they have not found widespread application in high temperature environments. When the operating temperature rises above 60°C, the device becomes unsafe because the boiling point of most of these organic solvents is below 80°C. As a result it is almost impossible for these secondary cells to be operated above 100°C [68]. Herein, we will debate the wide temperature range (including low and high temperatures) application of post-lithium ion batteries i.e., magnesium ion batteries [18,69].

Recently, in search of new alternatives, ionic liquids have emerged as ideal alternatives having a low vapor pressure, high thermal sta-

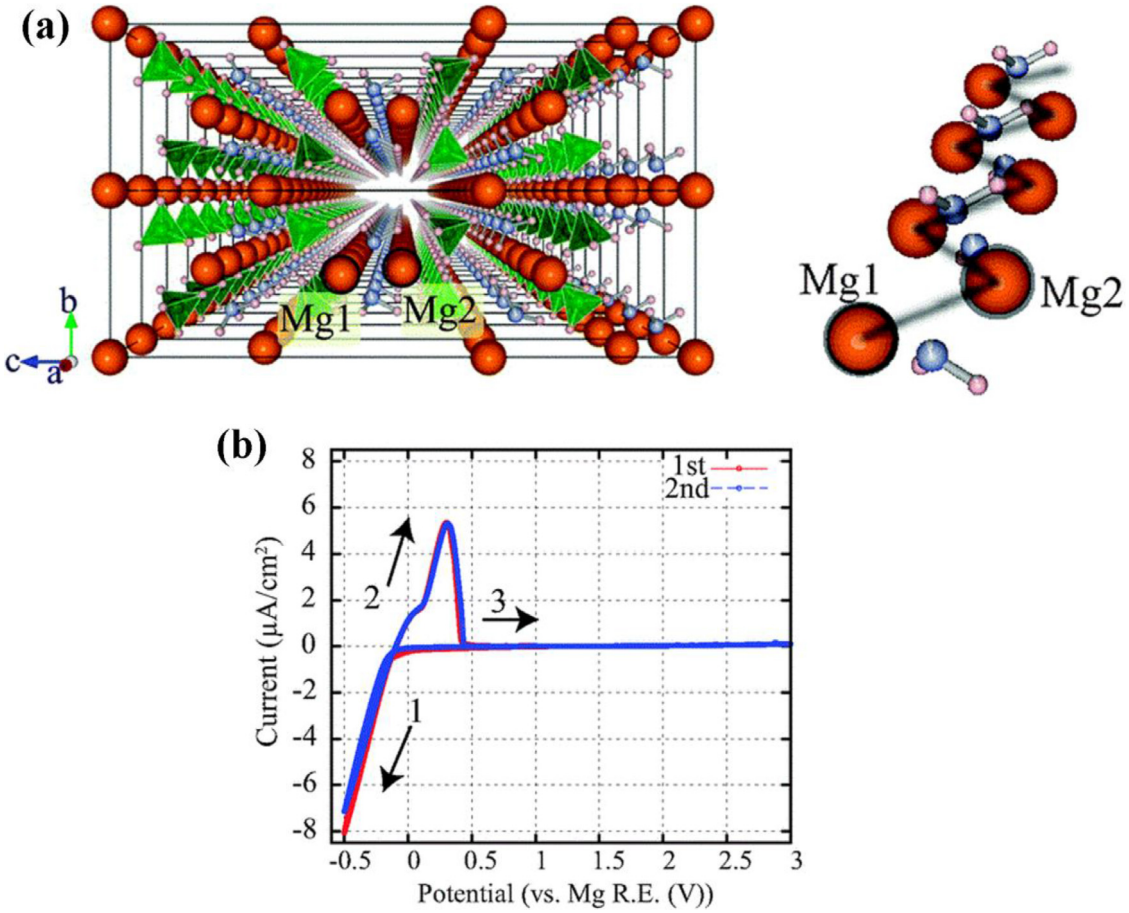


**Fig. 3.** b (a) Crystal structure of $Mg(BH_4)(NH_2)$ viewed along the a-axis and an enlarged image of the Mg-ion zigzag arrangement, and cyclic voltammograms of (b) Pt/$Mg(BH_4)(NH_2)$/Mg (Reproduced with permission from [62] Copyright (2013)).

bility, low toxicity, being non-flammable, and a large electrochemical potential window [70,71]. The advantages of low vapor pressure and high thermal stability offers the high penetration of the electrolyte into the electrode and makes the system safer while operating at high temperatures. Inspired by the potential advantages of vanadium pentoxide ($V_2O_5$), Novak et al. [72] made a successful attempt to accommodate the magnesium ions inside this host material. This further enhanced the reversible capacities by adding water contents into magnesium perchlorate-acetonitrile based electrolytes. The resultant improvement in the reversible capacities was attributed to the charge shielding effect of water dipoles that renovate the magnesium ion into solvated ion thus exhibiting reduced polarizations (Fig. 4a). Since the presence of water or moisture in magnesium electrolytes may passivate the magnesium anode surface, researchers have used cathode materials already containing water molecules intercalated inside the host materials crystal structure [73]. Unfortunately, such host materials exhibited rapid capacity fading owing to the removal of water from the crystal structure of the host material during redox reactions. Takeuchi et al. [74] attempted to fabricate the $Mg_{0.1}V_2O_5$ $1.8H_2O$ via a novel sol gel technique and tested for its performance as a cathode material in magnesium batteries. This cathode exhibited an excellent capacity of 280 mA h $g^{-1}$ because the water molecules in the structure coordinate to $Mg^{2+}$ as the solvation shell to effectively screen the divalent charge. Qinyu et al. [75] demonstrated that graphene decorated hydrated vanadium oxide nanocomposite can be an effective cathode material for wide temperature range magnesium ion storage. The cathode materials were prepared using a pre-formed vanadium pentoxide solution, reduced graphene oxide (rGO) suspension and $NH_4H_2PO_4$ at 80°C. Owing to the presence of electrostatic interactions inside precursor solutions, both graphene and vanadium pentoxide are self-assembled via growth of vanadium pentoxide nanowires inside graphene sheets supported by Ostwald ripening as depicted in Fig. 4a-b [75].

For electrochemical characterization, magnesium bis(trifluoromethane sulfonyl) imide ($Mg(TFSI)_2$)-acetonitrile based electrolyte solution was chosen along with activated carbon (AC) clothes to act as both counter electrode and quasi-reference electrode. Experimental results revealed that the synthesized composite exhibited a good cycle life with a capacity retention of 81% at 1.0 A $g^{-1}$ for 200 cycles (Fig. 4d). Furthermore, the coulombic efficiency preserved was greater than 99% during all the cycles and no change in shape of charging/discharging profiles was observed even after 200 cycles (Fig. 4e). More interestingly, the working potential of the charging/discharging curves was more than 2.5 V, significantly higher than state-of-the-art of magnesium batteries. The rate capability tests (with current densities ranging from 0.05 to 2.0 A $g^{-1}$) revealed that the cathode exhibited its highest capacity (320 mAh $g^{-1}$ at 0.05 A $g^{-1}$) to intercalate magnesium ions and when the current density was increased to a value of 2.0 A $g^{-1}$, a specific capacity of 100 mAh $g^{-1}$ was retained as shown in Fig. 4f-g. The magnesium battery was cycled at different temperatures such as 55, 40, 20, 0, –15, and –30°C, as shown in Fig. 4h. It was observed that the battery exhibited a specific capacity of 200 mAh $g^{-1}$ at 55°C when cycled at 1 A $g^{-1}$. This value is higher than the specific capacity (120 mAh $g^{-1}$) of the battery measured at room temperature and it was found that the reversible capacity increased with increases in temperature. When the temperature was lowered to a value of –30°C, a reversible capacity of 40 mAh $g^{-1}$ was retained by the magnesium battery. This suggests that the batteries capacity is affected by the magnesium ion diffusion, which may increase or decrease depending on the

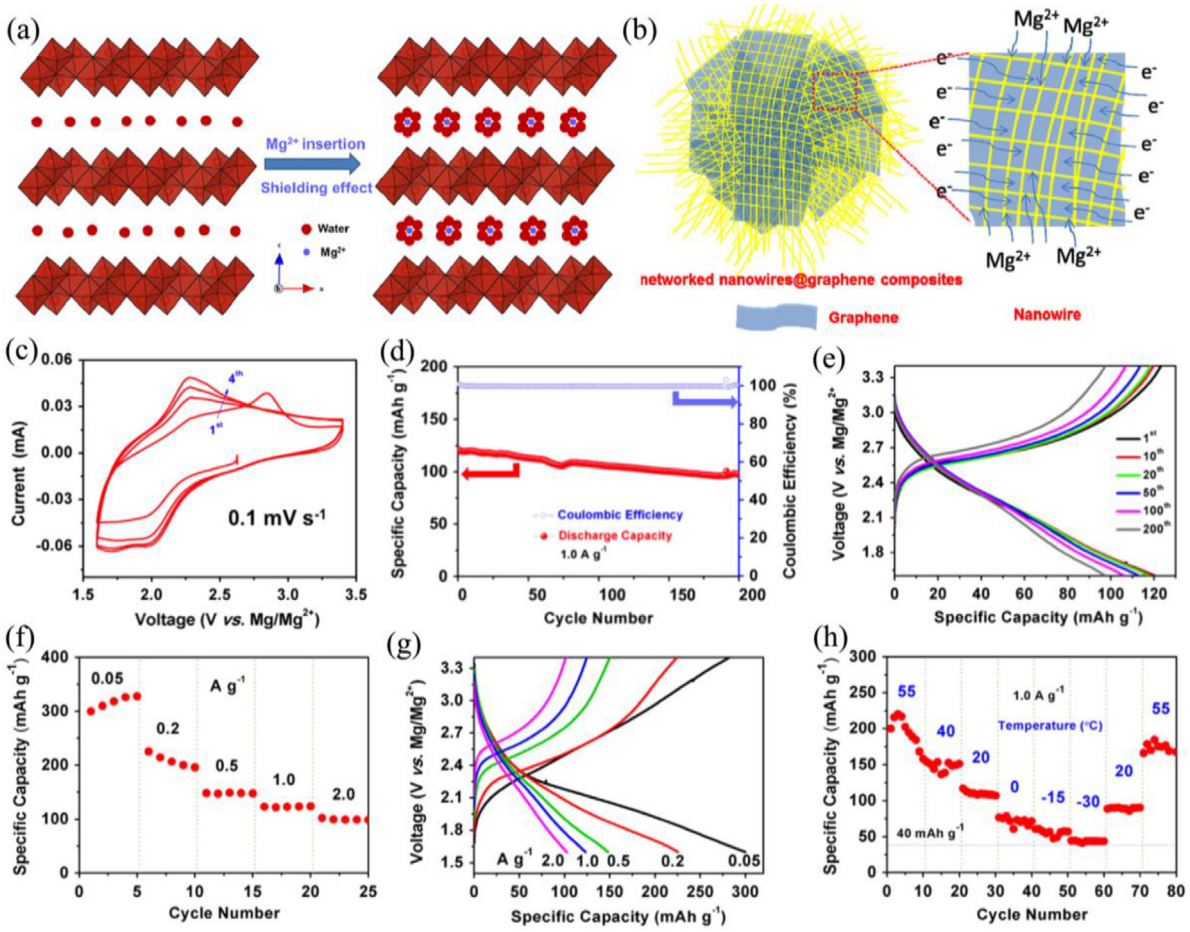


**Fig. 4.** (a) Shielding effect of $Mg^{2+}$ in the hydrated $V_2O_5$ $nH_2O$. The strong polarization of the divalent $Mg^{2+}$ could be significantly reduced by solvating with crystal water molecules, (b) Schematic illustration of the $V_2O_5$ $nH_2O$@rGO nanocomposite with bi-continuous electron/ion transport pathways, large area of electrode–electrolyte interface, and facile strain relaxation during $Mg^{2+}$ insertion/extraction, (c) Cyclic voltammograms of VOG-1 electrode between 1.6 and 3.4 V vs. $Mg/Mg^{2+}$ at a scan rate of 0.1 mV $s^{-1}$, (d) Cycling performance, (e) Charge–discharge profiles of VOG-1 at 1.0 A $g^{-1}$, (f) Rate performance, (g) charge–discharge profiles at various current density, and (h) Discharge capacity at various temperatures from –30 to 55°C at 1.0 A $g^{-1}$ (Reproduced with permission from [75] Copyright Elsevier (2015)).

environmental temperatures. This study for the first time revealed the capability of vanadium pentoxide-graphene composite to accommodate magnesium ions in a broad range of working temperature [75].

Apart from $V_2O_5$, the binary vanadium dioxides ($VO_2$) have received significant research interest owing to its various polymorphic configurations. To date about nine polymorphic forms of vanadium dioxides have been reported including rutile, monoclinic, triclinic, tetragonal, monoclinic, tetragonal, monoclinic, paramontroseite, and body centered cubic structures [76]. The binary vanadium dioxides can also be synthesized using $V_2O_5$ as precursors [76,77]. The transformation of $V_2O_5$ into $VO_2$ is shown in Fig. 5a. $VO_2$ has been extensively employed as a cathode material for rechargeable metal-ion batteries [78]. $VO_2$ displays uniform voltage platforms at about 2.5 V *vs.* $Li/Li^+$ and 1.75 V *vs.* $Mg/Mg^{2+}$, confirming its ability to deliver high energy densities. To investigate the capability of vanadium dioxides ($VO_2$) cathode for both low and high temperature applications, Pei et al. [77] synthesized nanorods and tested their performance in magnesium batteries. The synthesis of $VO_2$ nanorodes were carried out using hydrothermal reaction inside the Teflon-lined stainless steel autoclaves for 24 hours at 180°C. The reaction precursors used in their work were $V_2O_5$, $H_2C_2O_4{\bullet}2H_2O$, and polyethylene glycol 4000 dissolved inside the water. The synthesized nanorodes exhibited high crystallinity and uniform morphology (with ~100 nm in width, hundreds of nanometers in length and ~20 nm in thickness) as shown by microstructural characterizations in Fig. 5b-d [77].

Unlike the previous report [75], the all-phenyl-complex solution and magnesium metal was chosen as electrolytes and anode material, respectively. For the synthesis of all-phenyl-complex (APC) solution, aluminum trichlorides and phenyl-magnesium chloride salts were dissolved in a tetrahydrofuran solution inside a glove box. To increase the ionic conductivity of APC electrolytes, different molar contents of lithium chlorides were also introduced. Thus, the new working principle involves the dissolution of magnesium ions from a magnesium metal anode and the insertion of lithium ions into a vanadium oxide cathode during the discharge process and vice versa. Room temperature results revealed the presence of one pair of defined redox peaks at 1.9/1.75 V, which correspond to the charging/discharging voltage profiles. It was noticed that pristine APC based batteries exhibited very poor performance, owing to high resistance faced by magnesium ions during insertion into the vanadium oxide crystal structure. However, the electrolyte solution with APC-1M LiCl composition and 0.5-2.0 V potential window revealed good cycle stability up to 100 cycles as depicted in Fig. 5(e-f). Reversible capacity of 154.9 mA h $g^{-1}$ was retained after 100 cycles, which is equivalent to a capacity retention of about 75%. Similarly, the rate performance (current density ranging from 50-500 mA $g^{-1}$) results revealed the high capability of the cathode material to accommodate

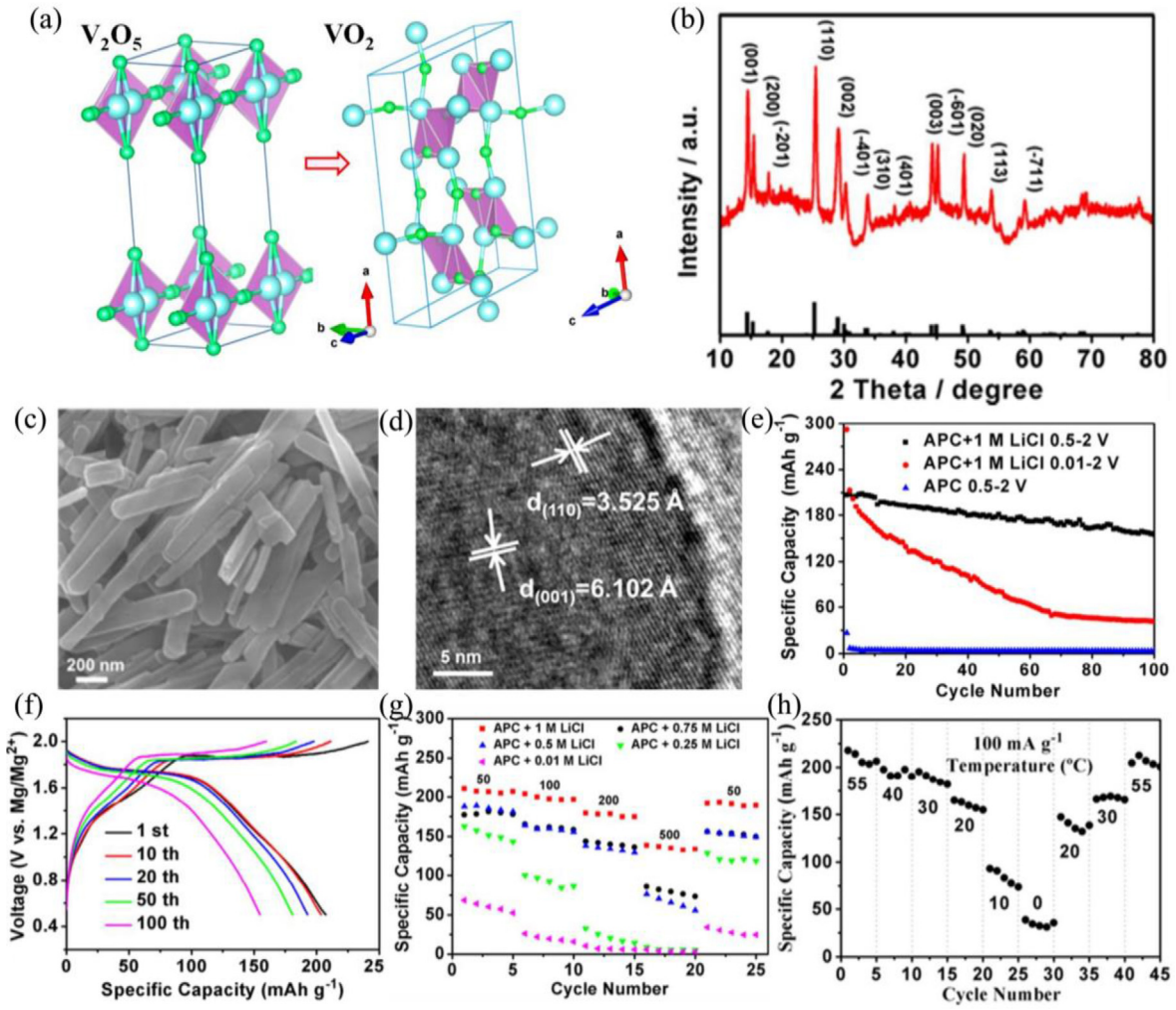


**Fig. 5.** (a) Polyhedral structures of orthorhombic $V_2O_5$ and monoclinic $VO_2$ (B), depicting the overall crystallographic transmutation occurring during the synthesis of the later. The Blue balls represent V atoms and the green balls represent the O atoms (Reproduced with permission from[76] Copyright RSC); (b) XRD patterns of $VO_2$, (c) FESEM images, (d) TEM images of the prepared $VO_2$, (e) Cycling performance of $VO_2$ cathode in MLIB with different electrochemical windows and $VO_2$ cathode in MIB at 20 mA g$^{-1}$, (f) Charge-discharge profiles of MLIB between the voltage window of 0.5–2 V, (g) Rate capability of $VO_2$ cathode, and (h) Discharge capacity at different temperatures between 0–55°C at 100 mA g$^{-1}$ (Reproduced with permission from [77] Copyright ACS (2017)).

guest ions. The cathode exhibited capacities of 210.6, 203.7, 179.6 and 138.3 mA h g$^{-1}$ at 50, 100, 200, and 500 mA g$^{-1}$, respectively (Fig. 5g). The reaction kinetics of the guest ion intercalation and deintercalation process determined the rate capability of the cathode. It also depends on the speed of electron transportation and diffusion path length. Other studies revealed that in hybrid ion systems, the capacity is dependent on both $Cl^-$ anion (effect on anodic stability) and $Li^+$ ion concentrations ($Li^+$ transference number) [79,80]. They also investigated the high and low temperature electrochemical performance of the vanadium oxide cathode in an environmental chamber. As shown in Fig. 5h, the system exhibited the discharge capacity of about 220 mA h g$^{-1}$ at 55°C, higher that the capacity measured at room temperature (206.8 mAh g$^{-1}$). However, when the temperature was decreased to freezing point (0°C), the battery exhibited the capacity of only 35 mAh g$^{-1}$, which revealed that decreasing temperature will slow the diffusion of guest ions inside the host cathode and vice versa. Furthermore, comparison of $V_2O_5$ and $VO_2$ performance at 0°C revealed that $V_2O_5$ outperform $VO_2$ owing to its high capability at low temperatures (facilitated by its unique lattice structure) [75,77].

Apart from orthorhombic $V_2O_5$ and monoclinic $VO_2$, 2D-ultrathin nanosheets-assembled spinel $MgIn_2S_4$ micorflowers (MIS-Fs) were also used to evaluate their electrochemical properties at high temperatures in magnesium ion batteries [81]. These MIS-Fs nanostructures were synthesized by solvothermal process, where different growth parameters (temperature (50 - 160 °C), reaction times) were also investigated to control the particle size of MIS-Fs. Synthesized material was casted onto platinum current collectors for cell assembly. For electrolyte preparation, ionic liquid 1-methyl-1-propylpyrrolidinium bis(trifluoromethanesulfonyl)imide ([MPPyr][TFSI]) was prepared followed by addition of Magnesium bis(trifluoromethanesulfonimide) ($Mg(TFSI)_2$) and tetraglyme (G4) in the ionic liquid ([MPPyr][TFSI]). The final $[Mg(G4)][TFSI]_2$ -[MPPyr][TFSI] solution with molar concentration of 0.3 M was used as an electrolyte. Assembled magnesium ion batteries (using a three-electrode system in a beaker cell) were tested using galvanostatic charging-discharging technique at elevated temperatures ranging from 50 to 150 °C with potential window of 1.2 – 3.2 V as shown in Fig. 6. Magnesium and Ag/Ag$^+$ were used as counter and reference electrodes, respectively.

Fig. 6a shows the galvanostatic voltage profiles measured at the current density of 20 mA g$^{-1}$ at the temperature range from 50 to 150°C. Interestingly, MIS-Fs cathode revealed the reversible capacities of about 235, 340, 450, and 500 mAh g$^{-1}$ at 50, 70, 100, and 150°C, respectively. It can be seen that voltage platforms (discharge) was observed at about 2 V against Mg/$Mg^{2+}$ at 150°C, which shifts towards lower

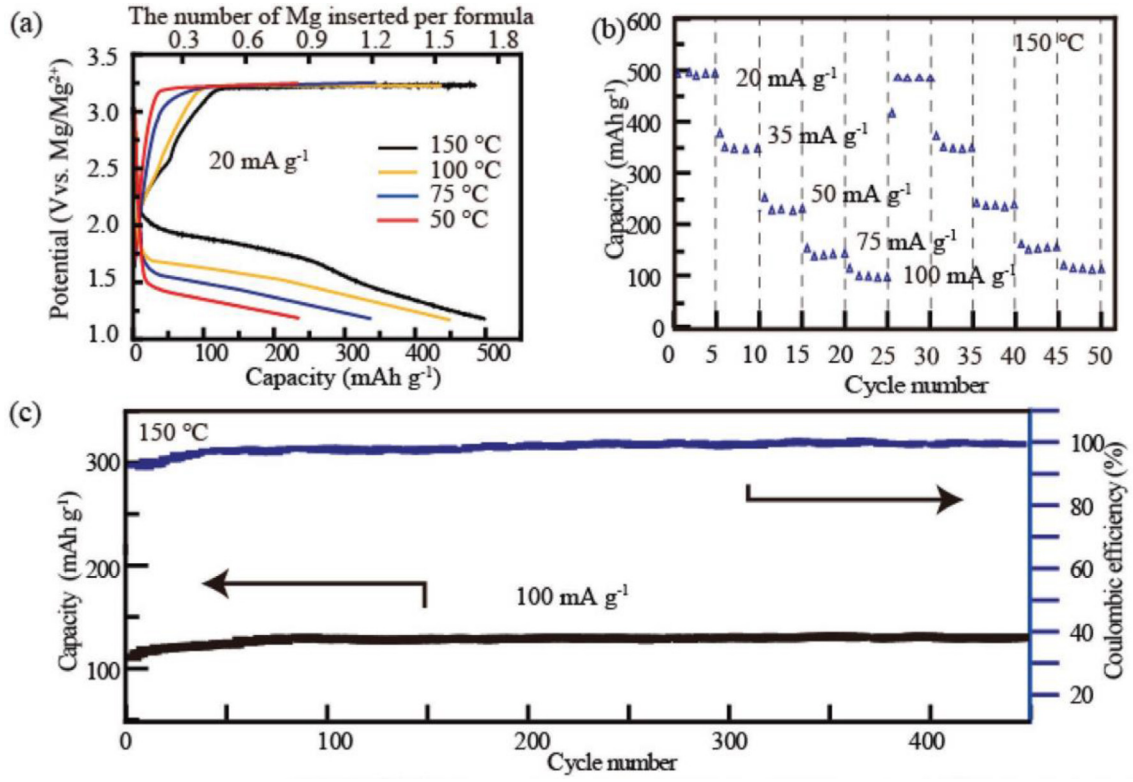


**Fig. 6.** Galvanostatic discharge-charge curves of MIS-F350 cathode in [Mg(G4)][TFSI]$_2$–[MPPyr][TFSI]. (a) Discharge–charge curves at different temperatures, (b) rate performance at different current densities of 20, 35, 50, 75, and 100 mA g$^{-1}$, and (c) long-term cycling performance at 100 mA g$^{-1}$ (Reproduced with permission from [81] Copyright Wiley (2019)).

values with decrease in temperatures. This confirms that discharge potential shifts to more anodic side with rise in temperature. The excellent reversible capacity and discharge potential were attributed to fast diffusions of $Mg^{2+}$ ions into nanostructured MIS-Fs cathode [82]. Inspired from high capacity of cathode, rate capability test was also conducted at shown in Fig. 6b. The reversible capacities of about 500, 350, 230, 180, and 130 mAh g$^{-1}$ were achieved at current densities of 20, 35, 50, 75, 100 mA g$^{-1}$, respectively. More importantly, capacity values were reserved back to original values after rate performance test, which shows the high capability of synthesized MIS-Fs cathode. Similarly, the cycle performance of MIS-Fs cathode exhibited excellent capacity retentions for 450 cycles at 100 mA g$^{-1}$ (Fig. 6c). These findings revealed that $MgIn_2S_4$ micorflowers outperform orthorhombic $V_2O_5$, monoclinic $VO_2$, and other cathodes by delivering high capacities at high temperatures (150°C). These improvements could be attributed to spinel sulfide structures and compositions of $MgIn_2S_4$ micorflowers [81].

The above results indicated the conversion reaction between $MgIn_2S_4$ and MgS, InS, and In in magnesiation and demagnesiation. Thus, the conversion reactions can be written as [81].

$$MgIn_2S_4 + 2Mg^{2+} + 4e^- \leftrightarrow 3MgS + InS + In \quad (1)$$

## 7. Low temperature electrochemistries

As, mostly hybrid ion electrolyte was used for low temperature studies. Therefore, before going into the low temperature studies, we will briefly discuss the concept of hybrid ion batteries and their pros and cons. Numerous attempts have been made to develop magnesium ion battery technology by exploring highly porous and high voltage host materials [10,13,64,65,69]. To bypass the sluggish magnesium ion transportation and take full benefit of the dendrite free cycling of magnesium metal anodes, the concept of hybrid ion batteries has emerged as a new strategy in recent years [36]. This can be achieved by introducing lithium or sodium ions inside the magnesium electrolytes with high intercalation capability with the host material. The working principle of a hybrid ion battery is shown in Fig. 7. During the discharge process, the magnesium dissolute from the metal magnesium anode, whereas lithium ions (present in hybrid electrolyte) will be diffused into the host cathode material. On the other hand, during the charge process the magnesium is deposited on magnesium anode and lithium ions are extracted from the cathode material. Since, lithium has a high compatibility with numerous host materials, high reversible capacities are expected. Despite this, the concept incorporates many advantages and disadvantages related with cathode materials, metal anodes, hybrid ion electrolytes, operating potential windows, and their compatibilities with each other, which are sketched below.

Firstly, unlike lithium metal anodes, the deposition and dissolution of magnesium ions on metal anode is very smooth, thus there is less possibility of dendrite formation. As there is low possibility of lithium deposition on the magnesium anode, the lithium ions occupy the cathode side and as a result high specific capacities can be achieved [18]. On the other hand, the cathode side of a hybrid ion system is occupied by fast insertion and extraction of highly compatible lithium ions. The fast magnesiation/demagnisiation of the anode and intercalation/deintercalation of the cathode will result in high rate and cycle stabilities, which will be superior than the pure magnesium ion batteries. Thirdly, the design of magnesium-lithium hybrid ion batteries gives rise to the possibility of utilizing conventional lithium cathodes (transition metal oxides, sulfides, phosphides, and polyanion cathodes), thus high specific capacities can easily be obtained [83].

Despite favorable advantages of hybrid-ion batteries, these systems also have several drawbacks in terms of their component incompatibilities. For example, magnesium-based hybrid ion batteries (either magnesium-lithium or magnesium-sodium) cannot afford the usage of magnesium perchlorate ($Mg(ClO_4)_2$) or magnesium

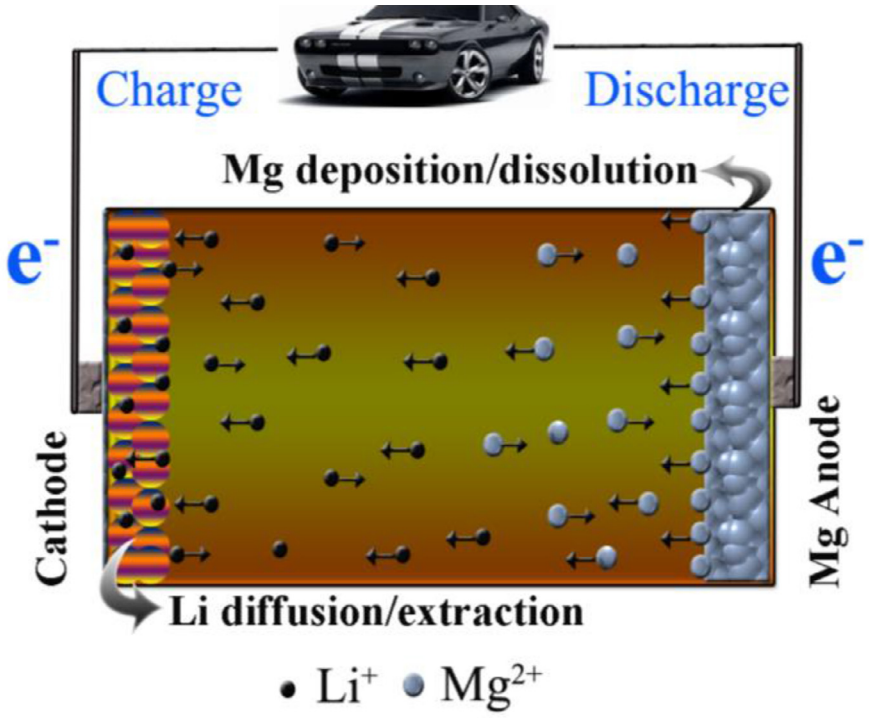


**Fig. 7.** Sketch diagram representing a Mg-Li hybrid ion battery: The battery consists of magnesium metal anode where deposition/dissolution of magnesium ions occurs and a transition metal oxide cathode, which is occupied by diffusion/extraction of $Li^+$ (or $Na^+$) ions during charging/discharging process (Reproduced with permission from [13] Copyright Elsevier (2020)).

bis(trifluoromethane sulfonyl) imide ($Mg(TFSI)_2$) salts dissolved in acetonitrile and carbonate based solvents, because these solutions will form a non-conducting passivation layer on anode surface, which will make magnesium deposition more difficult [84]. Furthermore, the quantity of electrolyte (which serves as ion reservoir to provide the $Li^+$ and $Mg^{2+}$ ions) needed for hybrid ion batteries is significantly higher, which will affect the weight of final battery. The choice of lithium salt is also crucial because many are insoluble or have limited solubility in magnesium electrolytes and the final hybrid electrolyte must be compatible with host materials to prevent side reactions. In addition, the anodic stability of magnesium electrolyte is affected by presence of lithium ions, i.e. presence of lithium ions inside the all-phenyl-complex electrolytes reduced the anodic stability to 2.5V [85].

Li-ion intercalation into graphite anodes is limited by high charge-transfer resistance at low environmental temperatures, leading to poor performance at low temperature for typicaly LIBs [86-88]. Furthermore the formation of potentially hazardous lithium dendrites is exacerbated, causing the cell to short circuit [89]. These issues cannot be ignored, as many fields such as aerospace and military missions require energy storage devices that can operated at ultra-low temperatures (for example –40°C). Magnesium ion technology can successfully operate at this temperature extremes and will be discussed in terms of the suitable electrolytes, cathodes and their underpinning operating mechanisms.

Zhang et al. [90] and his coworkers investigated the ultra-low temperature performance of magnesium-lithium hybrid ion battery for the first time. A conventional lithium cathode (lithium iron phosphate ($LiFePO_4$) was selected as the positive electrode (Fig. 8a) and magnesium metal was used as the negative/reference electrode. All-phenyl-complex (APC) electrolytes were prepared using aluminum chloride ($AlCl_3$) and phenyl-magnesium chloride (PhMgCl) salts dissolved in THF solvent. The molar concentration of APC solution was 0.5 M. To prepare the hybrid ion electrolyte, anhydrous LiCl was dissolved in an APC solution with concentrations ranging from 0 to 0.4 M [36]. Firstly, the cyclic voltammetry (CV) was used to examine the effect of lithium ion concentration on the electrochemistry of cell, which revealed an increase in both anodic and cathodic current intensities with increased lithium ion concentrations (0.5 M APC – 0.4 M LiCl revealed optimized performance). Thus, an optimized electrolyte solution was used for further electrochemical characterization both at room temperature and ultra-low temperatures. The pouch cell exhibited excellent cycle stability at room temperature, with an initial capacity of 103.9 mA h $g^{-1}$, which decreased to 102.4 mA h $g^{-1}$ after 200 cycles (capacity retention of 98.5%) as shown in Fig. 8b. The corresponding coulombic efficiency of the hybrid ion battery was maintained above 99.5%. Fig. 8c displays the rate performance of the battery at different current densities (0.15-3C). Careful observation reveals that the cathode exhibits very clear charge and discharge plateaus corresponding to the redox reaction of $Fe3^+/Fe^{2+}$. Compared with previous reports on magnesium batteries, the operating voltage of hybrid battery was significantly higher (about 2.5 V). Rate capability testing of the battery revealed specific capacities of 144.1, 123.2, 96.6, and 68.8 mA h $g^{-1}$ at a rate of 0.3, 0.6, 1.2, and 3.0C, respectively. The excellent performance of hybrid ion battery was attributed to the dendrite free cycling of the anode and fast reaction kinetics of lithium ion diffusion into the cathode. The lithium ion diffusion coefficient was found to be $1.67 \times 10^{-12}$ $cm^2$ $s^{-1}$ for $LiFePO_4$ cathode at room temperature. The high diffusion coefficient of lithium ions is favorable for high power density devices [90].

Moreover, the electrochemical performance for $LiFePO_4$ cathode based cells were tested at the low temperature range (0, – 10, – 20, and – 40°C). Firstly, the $LiFePO_4$ cathode was tested in a lithium ion battery (using traditional carbonate-based electrolytes), which revealed the best performance at temperatures above– 10°C. Then, the pouch cell hybrid ion battery was tested for cycle performance at 0, – 10, – 20, and – 40°C, for 50 cycles as shown in Fig. 8d-e. The magnesium-lithium hybrid ion battery and pure lithium ion battery delivered a maximum capacity of 103.5 and 109.8 mA h $g^{-1}$ at a temperature of 0°C, respectively. Careful analysis revealed that the hybrid ion battery exhibited reversible capacities of 109, 100, 90, and 80 mA h $g^{-1}$ at 0, – 10, – 20, and – 40°C, respectively without capacity fading. The excellent performance of hybrid ion battery at ultra-low temperature was attributed to the low viscosity and melting point of THF solvents, which resist against freezing of electrolyte solutions. With adequate operating potential (2.45 V) and energy density (382.2 W h $kg^{-1}$), this work laid the foundation for

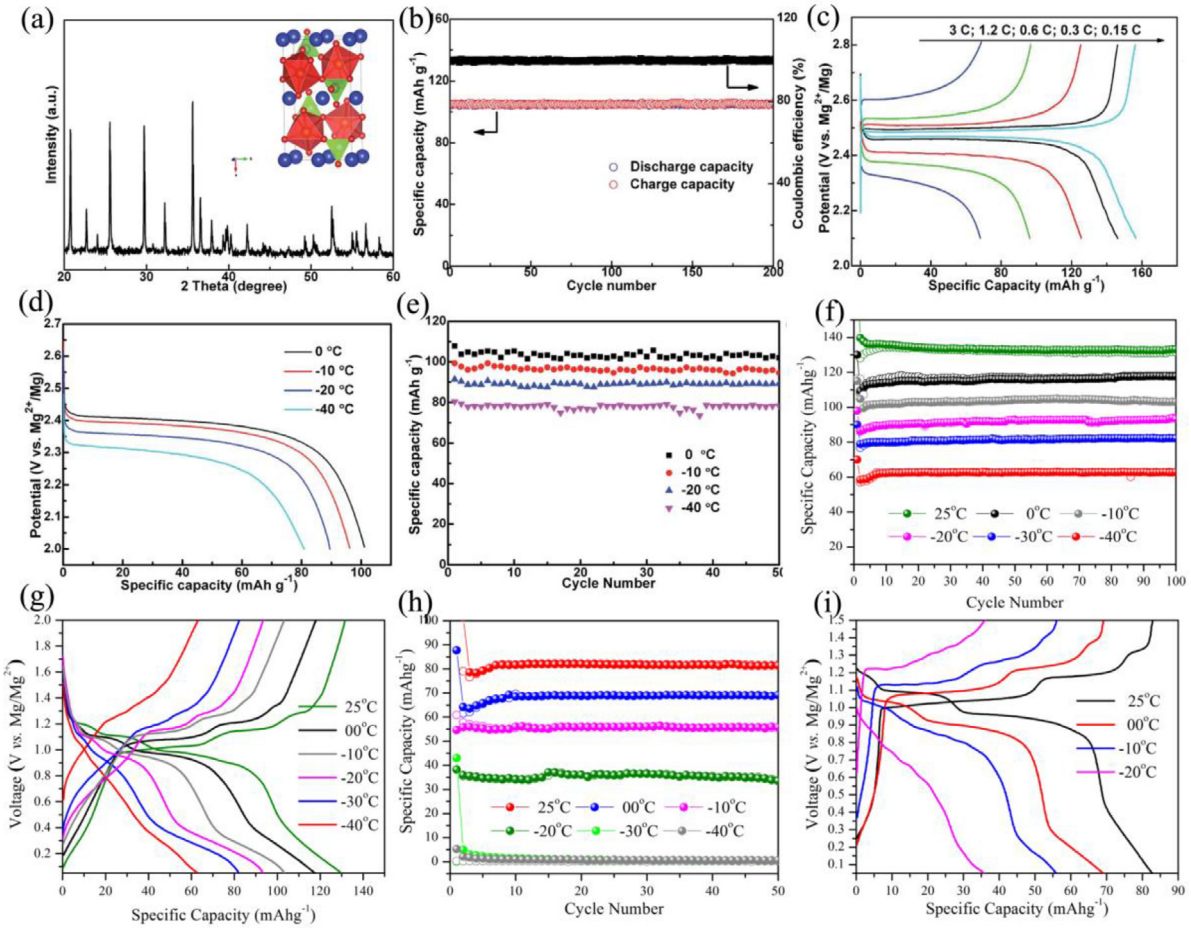


**Fig. 8.** (a) XRD pattern of the commercial LFP powder (inset: crystal structure of LFP), (b) Discharge–charge cycling performance and the corresponding coulombic efficiency of the LFP@GF electrode for hybrid $Mg^{2+}/Li^{+}$ batteries at room temperature, (c) Galvanostatic discharge–charge profiles of the rate performance at varied rates, Galvanostatic discharge–charge profiles (d) and cycling performance (e) of the hybrid $Mg^{2+}/Li^{+}$ battery at various low temperatures (Reproduced with permission from [90] Copyright RSC (2016)); (f) Cycle performance of LVP‖APC-LiCl‖Mg cells at RT and low temperatures (0, – 10, – 20, – 30, and – 40°C) at 100 mA $g^{-1}$ current rate, (g) Corresponding charge–discharge curves, (h) Cycle performance of LVP‖Mg/Li-BH‖Mg cells at RT and low temperatures (0, – 10, – 20, – 30, and – 40°C) at 100 mA $g^{-1}$ current rate, and (i) Corresponding charge–discharge curves (Reproduced with permission from [91] Copyright RSC (2019)).

magnesium-lithium hybrid ion batteries for ultra-low temperature applications [90].

In 2019, a polyanion $Li_3V_2(PO_4)_3$ (LVP) cathode was employed in magnesium-lithium hybrid ion batteries to evaluate the ultra-low temperature performance [91]. The synthesis of polyanion $Li_3V_2(PO_4)_3$ was carried out using a sol-gel technique [92]. The main precursors used in these experiments were $C_{12}H_{22}O_{11}$, $C_2H_2O_4$, $NH_4VO_3$, $Li_2CO_3$, and $NH_4H_2PO_4$. The synthesis of carbon coated $Li_3V_2(PO_4)_3$ was carried out at 350°C and 750°C (stepwise) in an argon atmosphere. Two kinds of hybrid ion electrolytes were prepared using optimized conditions. The synthesis of APC-LiCl/THF based electrolyte was carried out using previous reports [36,64,93]. The second kind of electrolyte was prepared in diglyme ($C_6H_{14}O_3$) (DG) with 0.1M of $Mg(BH_4)_2$ and 1.5M of $LiBH_4$ inside the glove box. Half-cells were assembled in glove box using magnesium metal as the anode, $Li_3V_2(PO_4)_3$ as cathode, and APC-LiCl/THF and Mg/Li-BH-based electrolyte solutions. Firstly, the electrochemical performance was evaluated at room temperature and later at ultra-low temperatures. Rate performance experiment of LVP‖APC-LiCl‖Mg and LVP‖Mg/Li-BH‖Mg cells at room temperature revealed the maximum capacities of 147 and 99.5 mA h $g^{-1}$, respectively at a current density of 50 mA $g^{-1}$. It was found that the APC-LiCl-based electrolyte outperformed the Mg/Li-BH solution, delivering reversible capacities of 147.8, 129, 114.4, 101.3, 87.4, and 65.3 mAh $g^{-1}$ at current densities of 50, 100, 250, 500, 1000, and 2500 mA $g^{-1}$, respectively. Mg/Li-BH based cell also exhibited excellent rate performance but specific capacities were lower compared to the APC-LiCl electrolyte. Interestingly, both kinds of cells exhibited voltage plateaus at about 1.0 V, which corresponds to the $Li^{+}$ ion intercalations/de-intercalation at LVP cathode during discharge/charge process and possible reaction mechanism can be expressed by Eqs. (2)–(4) [94,95].

$$Li_3V^{3+}V^{3+}(PO_4)_3 \rightarrow Li_{2.5}V^{3+}V^{3.5+}(PO_4)_3 + 0.5Li^{+} + 0.5e^{-} \quad (2)$$

$$Li_{2.5}V^{3+}V^{3.5+}(PO_4)_3 \rightarrow Li_2V^{3+}V^{4+}(PO_4)_3 + 0.5Li^{+} + 0.5e^{-} \quad (3)$$

$$Li_2V^{3+}V^{4+}(PO_4)_3 \rightarrow LiV^{4+}V^{4+}(PO_4)_3 + Li^{+} + e^{-} \quad (4)$$

Cycle stability testing revealed that capacity retentions for LVP‖APC-LiCl‖Mg and LVP‖Mg/Li-BH‖Mg half-cells were found to be 94.5 and 100%, respectively even after 200 cycles. The capacity decay of LVP‖APC-LiCl‖Mg half-cell was attributed to slow evaporation of THF from coin-cells during cycling [22]. After successful characterization of the $Li_3V_2(PO_4)_3$ cathode at room temperature, the half-cells were transferred to a low temperature chamber to check their capabilities at ultra-low temperatures. Fig. 8f-i depicts the electrochemical performance of half cells at 25, 0, – 10, – 20, – 30, and – 40°C for 100 cycles. The reversible capacities of 135, 117, 103.5, 93.4, 82.2, and 63.1 mA h $g^{-1}$ at 25, 0, – 10, – 20, – 30, and – 40°C, respectively were revealed by

APC-LiCl based electrolytes (Fig. 8f-g). It was noticed that sharpness of voltage plateaus decreases with temperature, owing to the slow transportation of guest ions. More importantly, the cells were able to preserve their initial capacity even after 100 cycles, revealing the high capability of APC-LiCl based electrolytes for low temperature applications. As discussed above, the main reasons for the observed performance improvements at ultra-low temperatures were the low viscosity and low melting point of THF, helping to reduce the freezing point of solutions. On the other hand, LVP‖Mg/Li-BH‖Mg half-cells exhibited good performance up to – 10°C owing to high boiling point of diglyme compared with that of THF as depicted in Fig. 8h-i. The cells exhibited specific capacities of 78, 69, 55.6, and 35 mA h $g^{-1}$ at 25, 0, – 10, and – 20°C, respectively. Further decreasing the temperature results in diglyme base electrolyte completely freezing and a capacity zero was achieved [91]. This work revealed that electrolyte solutions with low boiling points are ideal for devices used at ultra-low temperatures.

Lithium titanate ($Li_4Ti_5O_{12}$) has also emerged as a promising anode material owing to its low working potential, good cycle performance, and is considered an appealing alternative to graphite [96]. However, its poor electrical conductivity ($10^{-13}$ S.$cm^{-1}$) has restricted its use for practical applications [97]. Fortunately, the charge/discharge working potential of $Li_4Ti_5O_{12}$ lies in the range of magnesium electrolytes, thus can be used as anode in magnesium or magnesium-lithium hybrid ion batteries [98]. Despite several studies conducted on utilization of $Li_4Ti_5O_{12}$ electrode for magnesium batteries, little efforts have been made for low temperature electrochemical studies.

Recently, Rashad et al. [99] assembled magnesium-lithium hybrid ion battery using a $Li_4Ti_5O_{12}$ cathode, magnesium metal as anode, and APC-LiCl/THF based electrolytes. The working mechanism of the hybrid battery, morphology and crystal structure of LTO cathode are depicted in Fig. 9a-d. The electrochemistry of the battery was tested at different temperatures i.e. 25°C, 10°C, 0°C, – 10°C, and – 20°C. Experimental results revealed that the LTO cathode exhibited very poor specific capacity in pure APC/THF based electrolytes, which is attributed to the cathodes low electrical conductivity and sluggish magnesium ion transportations at room temperatures. On the other hand, when lithium ions were introduced into the magnesium electrolyte (APC-LiCl/THF), the specific capacities of 228, 212.5, 204.1, 199.7, 185.3 and 163 mA h $g^{-1}$ were achieved at the current densities of 20, 40, 100, 200, 400, and 1000 mA $g^{-1}$, respectively with stable voltage plateaus at 0.7/0.9 V, which corresponds to insertion/extraction of lithium ions into/from LTO cathode [99].

Inspired by the excellent room temperature performance, the half-cells were cycled at low temperatures (10°C, 0°C, – 10°C, and – 20°C) for CV measurements as shown in Fig. 9e. It was noticed that peak current intensities decrease, whereas the potential difference increase with decreasing temperatures. The main reason behind this change was slower guest ion transportation, resulting in reduced guest ions diffusion inside the LTO cathode at low temperatures. The LTO based hybrid ion cells were cycled at 25°C, 10°C, 0°C, – 10°C, and – 20°C for 50 cycles using a current density of 100 mA $g^{-1}$ as shown in Fig. 9f-g. The battery was able to deliver the specific capacities of 213.4, 165.5, 143.8, 133.2 and 78.56 mA h $g^{-1}$, at 25°C, 10°C, 0°C, – 10°C, and – 20°C, respectively. The voltage-capacity curve of batteries cycled at different temperatures were used to measure the polarizations, which increases with decreasing temperatures as depicted in Fig. 9h.

Determining the electrochemical polarization of rechargeable metal ion batteries at different temperature is very useful. This is because by employing electrochemical impedance spectroscopy (EIS) technique, one may understand origin of impedance features. Generally, it was noticed that temperature does not have a large effect on contact impedance compared with charge transfer resistance. Several reports showed that charge transfer resistance ($R_{ct}$) is highly dependent on temperatures [100]. The $R_{ct}$ is combination of gust ion desolvation and resistance required by guest ion to pass through SEI and enter into host material. Normally, desolvation part is very small and it can be neglected. Therefore, the main resistance contributing to electrochemical polarization is ion conduction via SEI. So the Arrhenius's Equation can represent the dependence of $R_{ct}$ on temperatures via following Eq. (5) [101].

$$\frac{1}{R_{ct}} = Ae^{-\left(E_a/k_BT\right)} \tag{5}$$

Where, $R_{ct}$ is the resistance faced by guest ion movement from electrolyte to electrode, $E_a$ is the activation energy related to guest ions, $k_B$ is the Boltzmann constant, A is proportionality constant, and T is the temperature. Therefore, by plotting the log of $R_{ct}$ vs. 1/T, we may estimate the activation energies associated with guest ion transportation between anode SEI and cathode SEI. The electrochemical impedance spectroscopy (EIS) technique was used to analyze the effect of temperature on the shape of Nyquist plots, which revealed an increase in charge transfer resistance at lower temperatures (Fig. 9i-j) [99]. This is because the diffusion coefficient of lithium ions (inside LTO cathode) decreases with lowering the environmental temperatures [99]. In conclusion, the $Li_4Ti_5O_{12}$ cathode is capable of operating efficiently down to a temperature of – 10°C using all-phenyl-complex based electrolyte solutions.

## 8. Stripping and plating behaviors of magnesium metal anode

Gradual discovering the mechanisms involved in the interphase of magnesium metal anode, stripping and plating of magnesium onto anode, chemical scientists found that surface of Mg metal anode facilitate the formation of artificial solid-electrolyte-interphase (SEI), which endorse the compatibility between anode surface and electrolyte species present in the systems [102,103]. From literature, we can see that Canepa et al. and his coworkers used first-principles calculations and ion-transport theory to investigate the several compounds as potential coating materials for Mg metal anodes [104,105]. In another work, an attempt was made to stabilize the Mg anode in the controversial $Mg(TFSI)_2$-based electrolyte via formation of the lithium containing SEI using an electrochemical cycling process [106]. Similarly, X. Li et al. [107] made successful attempt to minimize the overpotential values by making Mg anode based SEI using magnesium iodide layer on its surface. Germanium tetrachloride additive was also used in magnesium electrolytes to form in vivo Ge-based protective layer on magnesium surface, which exhibited self-repair effect during electrochemical cycling reactions [108]. Though, above discussed strategies (in situ generation of the interphase during the electrochemical process) showed promising results, however, it is very difficult to control the composition, thickness, mechanical and chemical properties of these as-formed SEI. Thus, simple and direct modifications of magnesium metal anode surface with the help of well-designed artificial coated materials could be more practicable for battery assembly. One such direct technique was employed by Ban et al. [109], who synthesized an electronic insulating and permeable (for $Mg^{2+}$ ions) artificial SEI on the surface of magnesium metal anode. This, artificial interphase exhibited high oxidation stability during reversible magnesium plating and stripping.

Inspired from above discussed works, Y. Zhao et al. [110] and his coworkers made successful attempt to modify the surface of magnesium metal anode using artificial layer of bismuth (Bi). This modification was carried out using a facile solution base approach, where targeted material was soaked into solution of bismuth trichlorides. The artificial protective layer was found to be consist of bismuth metal (with capability of conduct ions), magnesium-bismuth alloy, and electronically insulated magnesium chloride. Y. Zhao et al. [110] adopted various characterization and testing techniques to investigate the capability of artificial layer. It was observed that artificial layer on magnesium anode helps to prevent the occurrence of side reactions between magnesium metal and electrolyte species (non-corrosive). As a result, an uneven and dendrite like magnesium, plating and striping were suppressed [110].

While investigating the magnesium striping and platting mechanisms, Pint et al. [111] found that 3D hemispherical electrodeposition of magnesium was observed in $Mg(TFSI)_2$-DME based electrolytes,

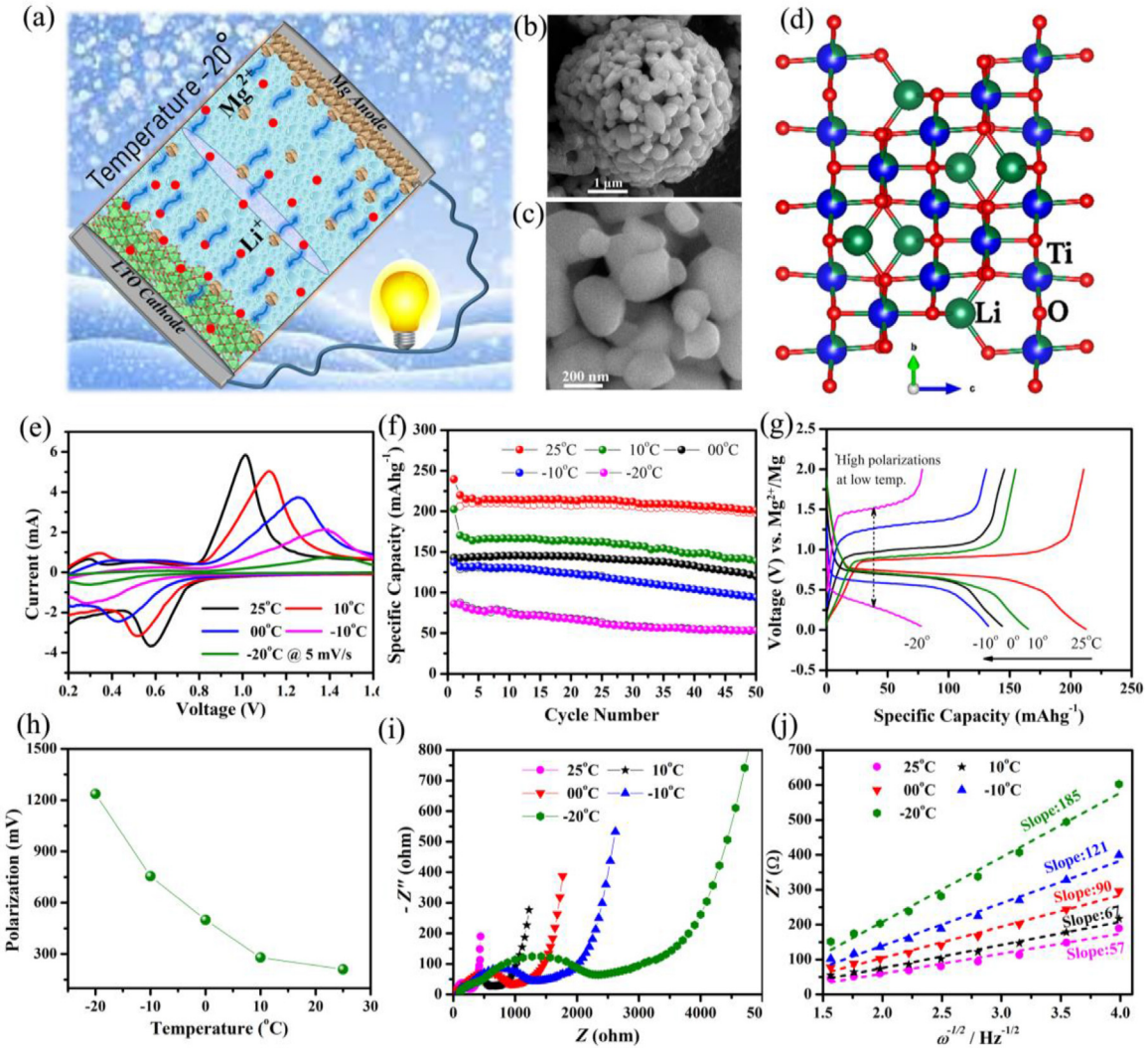


**Fig. 9.** (a) Sketch showing the working mechanism of Mg-Li hybrid battery at low temperature, (b-c) SEM images showing the structural morphologies of $Li_4Ti_5O_{12}$ spheres at different magnifications, (d) Refined crystal structure of $Li_4Ti_5O_{12}$, (e) CV curves measured at different temperatures, (f) cycle stabilities of half-cells measured at different temperatures (25, 10, 0, – 10, and – 20°C), (g) galvanostatic charging-discharging curves at different temperatures, (h) relation between polarizations of cells at different temperatures, Electrochemical impedance spectroscopy data of LTO cell in 0.4APC–1.0LiCl electrolyte. (i) Comparison of Nyquist plots at different temperatures (25, 10, 0, – 10, and – 20°C) showing the surface layer and the charge transfer resistance components, and (j) relation between Z' and $\omega^{-1/2}$ at different temperatures (Reproduced with permission from [99] Copyright Elsevier (2021)).

which led to shorting of magnesium ion batteries. Similarly, Zhao et al. [110] observed the growth of uneven magnesium depositions in $Mg(TFSI)_2$-DME based electrolytes in 2032-type coin type magnesium cells. For example, it can be observed in Fig. 10a that pristine (un-protected) magnesium-magnesium symmetric coin cells exhibited a large overpotential of about 2.0 V during initial charging-discharging process followed by abrupt fall in overpotential values just after eight cycles. Generally, vertical drop of overpotentials in symmetric cells represents an indication of shorting of cell [111]. Similar behavior was observed for other symmetric magnesium-magnesium coin cells, where overpotential drops to almost 0 V after two hours. On the other hand, protected magnesium-magnesium symmetric coil cells revealed an overpotential value of about ~ 0.6 V, which remained constant for about 4000 hours as shown in Fig. 10b. When using similar discharge conditions for another protected symmetric magnesium-magnesium coin cell, the duration time was found to be improved to 24 hours. Furthermore, images taken by operando optical microscopy for pristine and protected magnesium (during electroplating) are shown in Fig. 10c-d. It can be observed that during plating-stripping process, uneven magnesium is deposited and in some area, magnesium deposition is grown into humps along the tips when using pristine magnesium surface. On contrary, the magnesium anode protected with artificial layer revealed even depositions. Such growth patterns were further confirmed by SEM analysis as shown in Fig. 10e-h. It can be seen that mobs of uneven Mg deposits had formed on the pristine magnesium anode surface, whereas surface of protected magnesium anode presented uniform and dense morphology (with even surface) of deposited magnesium. From these findings, Zhao et al. [110] concluded that Mg-Mg symmetric coin cell can be inhibited from short-circuiting owing to presence of magnesium chloride inside bismuth based protecting layer.

## 9. Conclusions and future outlook

Though LIBs are already commercialized, they are unable to fulfill all future energy storage requirements due to the ever-increasing demand of energy storage devices in the market and limited lithium reservoirs. Rechargeable magnesium-ion batteries are one of the most favorable substitutes of the state-of-the-art lithium-ion batteries with numerous advantages over lithium technology. Extensive research has been carried out to optimized the magnesium-ion batteries in recent decades

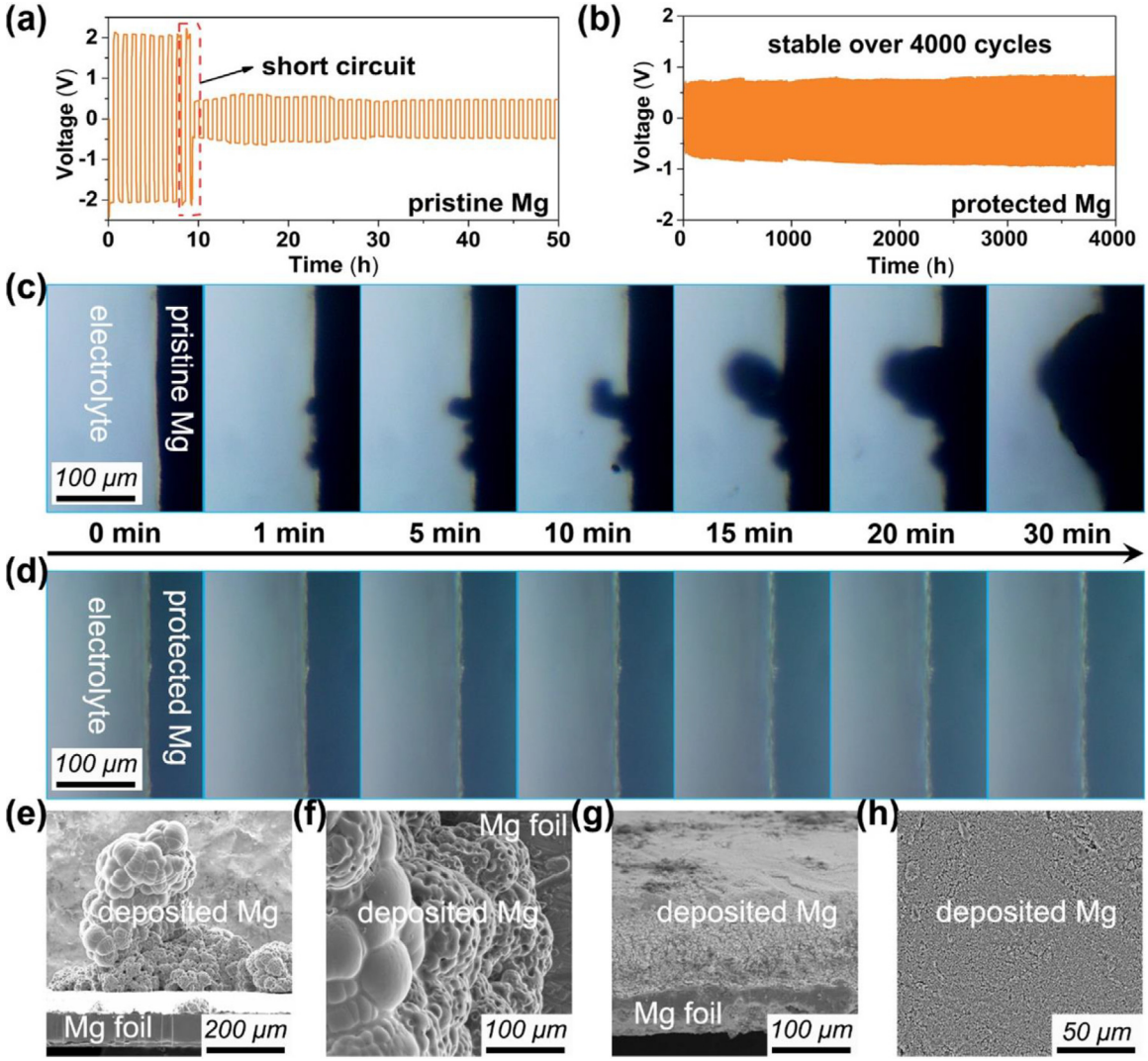


**Fig. 10.** (a, b) Cycling performance of symmetric Mg-Mg cells using the pristine Mg (a) and protected Mg (b) with 1 mA $cm^{-2}$, 0.5 mAh $cm^{-2}$. These data were obtained in 2032-type coin cells. (c, d) Operando optical microscope photographs taken with the increasing electroplating time of the pristine Mg (c) and the protected Mg (d) at 1 mA $cm^{-2}$. (e-h) Surface and cross-sectional SEM images of the pristine Mg (e, f) and the protected Mg (g, h) after electroplating Mg for 4 h at 1 mA $cm^{-2}$ (Reproduced with permission from [110] Copyright ACS (2021)).

with a number of notable breakthroughs. Apart from room temperature magnesium ion storage, the electrochemical performance of batteries at high and ultra-low temperatures has been investigated in recent years. Electrochemistry of the magnesium-ion batteries were greatly improved at extreme environmental conditions by tailoring the host cathodes, tuning the reference electrodes, and chemical hybridizations of both nucleophilic and non-nucleophilic electrolytes. In this review, we discussed extensive research efforts about the recent advances of magnesium-ion batteries working under extreme environmental conditions with higher voltage and better reversibility. According to the aforementioned advancements, the possible leading trends on wide temperature range (+ 150°C to – 40°C) magnesium-ion batteries and research space to fully meet the practical demands are listed below:

Design of novel host materials with fast diffusion kinetics for magnesium ions, a large operating voltage range, and retaining high specific capacities at elevated temperatures are still a great challenge for researchers. According to the aforementioned discussion, it was found that vanadium pentoxide, vanadium dioxide, and magnesium indium sulfide have been considered as promising cathode materials with high capabilities to store magnesium ions at high temperatures (up to + 150°C). Among these materials, magnesium indium sulfide exhibited highest performance in terms of reversible capacity and operating temperature i.e. + 150°C. These host oxide materials exhibited higher operating voltages compared to conventional room temperature magnesium-ion batteries. Thus, future research should be carried out on other metal sulfides (compatible with magnesium ion batteries) to study their capabilities to store magnesium ions at high temperatures. More research attention should be given to high voltage vanadium oxide-based cathodes to achieve high energy and power densities of final magnesium ion batteries at high temperatures.

For high temperature electrolyte solutions, the common cations and anions are alkylpyridinium, alkylpyrrolidinium, alkylpyrazolium, alkylimidazolium, etc. and $PF_6^-$, $BF_4^-$, $TFSI^-$ etc., respectively, which could be used for wide temperature range batteries. For example, the magnesium bis(trifluoromethane sulfonyl) imide ($Mg(TFSI)_2$)-acetonitrile based electrolyte solution was found to be suitable for high temperature energy storage. However, for acetonitrile-based electrolytes, the reference electrode should be activated carbon cloths or conventional anode materials instead of magnesium metal owing to its passivation. From this review work, we can concluded that ionic liquid i.e. 1-methyl-1-propylpyrrolidinium bis(trifluoromethanesulfonyl)imide ([MPPyr][TFSI])-$Mg(TFSI)_2$)-

tetraglyme (G4) based magnesium electrolytes are highly capable to execute high temperature electrochemical reactions even up to 150°C in magnesium-ion batteries. Therefore, future research should be focused on utilization of MPPyr-TFSI based electrolyte solutions with new compatible host materials to store the magnesium ions at high temperatures. High reversible capacities are expected to be achieved using these electrolytes at high temperatures. On contrary, all-phenyl-complex (APC) electrolytes can be used at room temperatures. This is because the boiling point of tetrahydrofuran solvent is very low; it may result in capacity decay due to its evaporation at high temperatures.

Since sluggish magnesium ion diffusion kinetics greatly hinders the achievement of high specific capacities, attempts were made to bypass slow magnesium ion transportation inside the host cathode. Introducing small amounts of lithium ions inside the magnesium electrolyte may boost the specific capacities and reaction kinetics. It may also increase the possibility of using conventional lithium cathodes. For example, APC-LiCl/THF and Mg/Li-BH/DG solutions exhibited good electrochemical performance both at room temperature and ultra-low temperatures (– 40°C). It was found that APC-LiCl/THF outperformed the Mg/Li-BH/DG solutions owing to its high ionic conductivities and low boiling point of THF compared to that of DG. From these works, we can conclude that APC-THF electrolytes are suitable for low temperature applications. Since, hybrid ion electrolytes have several drawbacks (i.e. mass/volume losses, ionic conductivities, lower working voltages, and side reactions etc.). Thus, attempts should be made by chemical researchers to examine the capabilities of APC-THF based pristine magnesium electrolytes with compatible electrodes at ultra-low temperatures.

Development of hybrid ion batteries have omitted the focus on cathode designs and tailoring of nanostructures because conventional lithium cathodes could be employed to achieve high energy densities. At ultra-low temperatures polyanion materials such as $LiFePO_4$, $Li_3V_2(PO_4)_3$, and $Li_4Ti_5O_{12}$ have been extensively used in rechargeable magnesium ion batteries. Among these cathodes, $LiFePO_4$ was able to yield acceptable energy densities (382.2 W h $kg^{-1}$) at the temperature of – 40°C using APC-LiCl/THF based electrolytes. Thus, future research should be focused on $FePO_4$-based magnesium cathode with pristine magnesium electrolytes to achieve practicable energy density at low temperatures.

In short, the commercialization of high performance rechargeable magnesium ion batteries with stable capability and fast reaction kinetics (at high and ultra-low temperatures) could be achieved by devoting more research attention to explore the promising cathode materials and compatible electrolytes.

## Declaration of Competing Interest

There is no conflict of interest.

## Acknowledgments

We acknowledge university of limerick to carry out this work.

## References

[1] R. Xiong, et al., Lithium-ion battery aging mechanisms and diagnosis method for automotive applications: recent advances and perspectives, Renewable Sustainable Energy Rev. 131 (2020) 110048.
[2] P. Lyu, et al., Recent advances of thermal safety of lithium ion battery for energy storage, Energy Storage Mater. 31 (2020) 195–220.
[3] M. Asif, et al., Confined polysulfide shuttle by nickel disulfide nanoparticles encapsulated in graphene nanoshells synthesized by cooking oil, ACS Appl. Energy Mater. 3 (4) (2020) 3541–3552.
[4] M. Asif, M. Rashad, Z. Ali, Electrochemical intercalations of divalent ions inside Ni/Zn co-doped cobalt sulfide nanoparticle decorated carbon spheres with superior capacity, Nanoscale 12 (26) (2020) 14267–14278.
[5] M. Asif, et al., Synthesis of ternary metal oxides as positive electrodes for Mg–Li hybrid ion batteries, Nanoscale 12 (2) (2020) 924–932.
[6] M. Rashad, M. Asif, Solid-state synthesis of nitrogen-doped graphitic nanotubes with outstanding electrochemical properties, Arabian J. Chem. 14 (5) (2021) 103113.
[7] B.H. Hou, et al., N-doped carbon-coated Ni<inf>1.8</inf>Co<inf>1.2</inf>Se<inf>4</inf encapsulated in N-doped carbon nanoboxes as advanced anode with outstanding high-rate and low-temperature performance for sodium-ion half/full batteries, Adv. Funct. Mater. (47) (2018) 28.
[8] Z. Liu, et al., Advances and perspectives on transitional metal layered oxides for potassium-ion battery, Energy Storage Mater. 34 (2021) 211–228.
[9] T.-T. Wei, et al., Advancement of technology towards high-performance non-aqueous aluminum-ion batteries, J. Energy Chem. (2020).
[10] M. Rashad, M. Asif, Z. Ali, Quest for magnesium-sulfur batteries: current challenges in electrolytes and cathode materials developments, Coord. Chem. Rev. 415 (2020) 213312.
[11] J. Emsley, in: Nature's Building Blocks An A-Z Guide to the Elements, Oxford University Press, Oxford, 2011, p. 699.
[12] Y. Orikasa, et al., High energy density rechargeable magnesium battery using earth--abundant and non-toxic elements, Sci. Rep. 4 (1) (2014) 5622.
[13] M. Rashad, et al., Recent advances in electrolytes and cathode materials for magnesium and hybrid-ion batteries, Energy Storage Mater. 25 (2020) 342–375.
[14] C. Yan, et al., Highly dispersed Zn nanoparticles confined in nanoporous carbon network: promising anode materials for sodium and potassium ion batteries, J. Mater. Chem. A (2018).
[15] B.C. B, in: Challenges of a Rechargeable Magnesium Battery A Guide to the Viability of this Post Lithium-Ion Battery, 11, Springer, Cham, 2018, p. 11.
[16] M. Rashad, M. Asif, Controlled synthesis of hierarchical porous carbons with different morphologies and their application for potassium and lithium ion batteries, New J. Chem. (2021).
[17] M. Rashad, M. Asif, Recycling Biowaste to synthesize nitrogen-doped highly porous activated carbon scaffolds for selenium stuffing with superior electrochemical properties, ACS Appl. Energy Mater. 4 (3) (2021) 2786–2796.
[18] M. Asif, et al., Ni-doped MnO2/CNT nanoarchitectures as a cathode material for ultra-long life magnesium/lithium hybrid ion batteries, Mater. Today Energy 10 (2018) 108–117.
[19] M. Rashad, et al., Low-cost room-temperature synthesis of NaV3O8•1.69H2O nanobelts for Mg batteries, ACS Appl. Mater. Interfaces 10 (5) (2018) 4757–4766.
[20] Z. Lu, et al., On the electrochemical behavior of magnesium electrodes in polar aprotic electrolyte solutions, J. Electroanal. Chem. 466 (2) (1999) 203–217.
[21] D. Aurbach, et al., Prototype systems for rechargeable magnesium batteries, Nature 407 (2000) 724.
[22] D. Aurbach, et al., Progress in rechargeable magnesium battery technology, Adv. Mater. 19 (23) (2007) 4260–4267.
[23] T.D. Gregory, R.J. Hoffman, R.C. Winterton, Nonaqueous electrochemistry of magnesium: applications to energy storage, J. Electrochem. Soc. 137 (3) (1990) 775–780.
[24] M. Rashad, et al., Fast kinetics of Mg2+/Li+ hybrid ions in polyanion Li3V2(PO4)3 cathode in wide temperature range, J. Mater. Chem. A (2019).
[25] J. Muldoon, et al., Electrolyte roadblocks to a magnesium rechargeable battery, Energy Environ. Sci. 5 (3) (2012) 5941–5950.
[26] V. Armel, et al., Organic ionic plastic crystal electrolytes; a new class of electrolyte for high efficiency solid state dye-sensitized solar cells, Energy Environ. Sci. 4 (6) (2011) 2234–2239.
[27] S.-J. Kang, et al., Non-grignard and lewis acid-free sulfone electrolytes for rechargeable magnesium batteries, Chem. Mater. 29 (7) (2017) 3174–3180.
[28] O. Tutusaus, et al., An efficient halogen-free electrolyte for use in rechargeable magnesium batteries, Angew. Chem. 127 (27) (2015) 8011–8015.
[29] C. Liebenow, Z. Yang, P. Lobitz, The electrodeposition of magnesium using solutions of organomagnesium halides, amidomagnesium halides and magnesium organoborates, Electrochem. Commun. 2 (9) (2000) 641–645.
[30] D. Aurbach, et al., Electrolyte solutions for rechargeable magnesium batteries based on organomagnesium chloroaluminate complexes, J. Electrochem. Soc. 149 (2) (2002) A115.
[31] N. Amir, et al., Progress in nonaqueous magnesium electrochemistry, J. Power Sources 174 (2) (2007) 1234–1240.
[32] O. Mizrahi, et al., Electrolyte solutions with a wide electrochemical window for rechargeable magnesium batteries, J. Electrochem. Soc. 155 (2) (2008) A103.
[33] Y. Guo, et al., Study of electronic effect of Grignard reagents on their electrochemical behavior, Electrochem. Commun. 12 (12) (2010) 1671–1673.
[34] P.K. Nayak, et al., From lithium-ion to sodium-ion batteries: advantages, challenges, and surprises, Angew. Chem. Int. Ed. 57 (1) (2018) 102–120.
[35] C.P. Grey, J.M. Tarascon, Sustainability and in situ monitoring in battery development, Nat. Mater. 16 (1) (2017) 45–56.
[36] M. Rashad, X. Li, H. Zhang, Magnesium/lithium-ion hybrid battery with high reversibility by employing NaV3O8•1.69H2O nanobelts as a positive electrode, ACS Appl. Mater. Interfaces 10 (25) (2018) 21313–21320.
[37] Z. Zhang, et al., Rechargeable magnesium batteries using conversion-type cathodes: a perspective and minireview, Small Methods 2 (10) (2018) 1800020.
[38] D. Aurbach, et al., Prototype systems for rechargeable magnesium batteries, Nature 407 (6805) (2000) 724–727.
[39] J. Muldoon, C.B. Bucur, T. Gregory, Quest for nonaqueous multivalent secondary batteries: magnesium and beyond, Chem. Rev. 114 (23) (2014) 11683–11720.
[40] H.D. Yoo, et al., Mg rechargeable batteries: an on-going challenge, Energy Environ. Sci. 6 (8) (2013) 2265–2279.
[41] P. Canepa, et al., Odyssey of multivalent cathode materials: open questions and future challenges, Chem. Rev. 117 (5) (2017) 4287–4341.
[42] J. Muldoon, C.B. Bucur, T. Gregory, Fervent hype behind magnesium batteries: an open call to synthetic chemists—electrolytes and cathodes needed, Angew. Chem. Int. Ed. 56 (40) (2017) 12064–12084.

[43] Z. Zhao-Karger, M. Fichtner, Magnesium–sulfur battery: its beginning and recent progress, MRS Commun. 7 (4) (2017) 770–784.
[44] H. Tian, et al., High power rechargeable magnesium/iodine battery chemistry, Nat. Commun. 8 (1) (2017) 14083.
[45] X. Yao, et al., A rechargeable non-aqueous Mg-Br2 battery, Nano Energy 28 (2016) 440–446.
[46] M.M. Huie, et al., Cathode materials for magnesium and magnesium-ion based batteries, Coord. Chem. Rev. 287 (2015) 15–27.
[47] D. Kundu, et al., A high-capacity and long-life aqueous rechargeable zinc battery using a metal oxide intercalation cathode, Nat. Energy 1 (10) (2016) 16119.
[48] S. Ikeda, et al., Solid electrolytes with multivalent cation conduction. 1. Conducting species in Mg Zr PO4 system, Solid State Ion. 23 (1) (1987) 125–129.
[49] S. Higashi, et al., A novel inorganic solid state ion conductor for rechargeable Mg batteries, Chem. Commun. 50 (11) (2014) 1320–1322.
[50] P. Canepa, et al., High magnesium mobility in ternary spinel chalcogenides, Nat. Commun. 8 (1) (2017) 1759.
[51] X. Sun, et al., A high capacity thiospinel cathode for Mg batteries, Energy Environ. Sci. 9 (7) (2016) 2273–2277.
[52] D. Sheppard, R. Terrell, G. Henkelman, Optimization methods for finding minimum energy paths, J. Chem. Phys. 128 (13) (2008) 134106.
[53] M. Adamu, G.M. Kale, Novel sol–gel synthesis of MgZr4P6O24 composite solid electrolyte and newer insight into the Mg2+-ion conducting properties using impedance spectroscopy, J. Phys. Chem. C 120 (32) (2016) 17909–17915.
[54] N. Imanaka, Y. Okazaki, G.-y. Adachi, Divalent magnesium ion conducting characteristics in phosphate based solid electrolyte composites, J. Mater. Chem. 10 (6) (2000) 1431–1435.
[55] P.W. Jaschin, et al., A materials perspective on magnesium-ion-based solid-state electrolytes, J. Mater. Chem. A 8 (6) (2020) 2875–2897.
[56] Z.A. Halim, S.B.R.S. Adnan, N.S. Mohamed, Effect of sintering temperature on the structural, electrical and electrochemical properties of novel Mg0.5Si2 (PO4)3 ceramic electrolytes, Ceram. Int. 42 (3) (2016) 4452–4461.
[57] Z.A. Halim, et al., Effects of Mg2+ interstitial ion on the properties of Mg0.5+x/2Si2-xAlx(PO4)3 ceramic electrolytes, J. Magn. Alloys 5 (4) (2017) 439–447.
[58] M. Sulaiman, N.Che Su, N.S. Mohamed, Sol-gel synthesis and characterization of $\beta$-MgSO4:Mg(NO3)2–MgO composite solid electrolyte, Ionics 23 (2) (2017) 443–452.
[59] A. Omote, et al., High ion conductivity in MgHf(WO4)3 solids with ordered structure: 1-D alignments of Mg2+ and Hf4+ ions, J. Am. Ceram. Soc. 94 (8) (2011) 2285–2288.
[60] M. Matsuo, et al., Sodium and magnesium ionic conduction in complex hydrides, J. Alloys Compd. 580 (2013) S98–S101.
[61] A. Unemoto, M. Matsuo, S.-i. Orimo, Complex hydrides for electrochemical energy storage, Adv. Funct. Mater. 24 (16) (2014) 2267–2279.
[62] R. Mohtadi, et al., Magnesium borohydride: from hydrogen storage to magnesium battery, Angew. Chem. Int. Ed. 51 (39) (2012) 9780–9783.
[63] Q. Guo, et al., Recent developments on anode materials for magnesium-ion batteries: a review, Rare Met. (2020).
[64] M. Rashad, et al., Quest for carbon and vanadium oxide based rechargeable magnesium-ion batteries, J. Magn. Alloys (2020).
[65] M. Rashad, S.D.A. Zaidi, M. Asif, Debating the magnesium–selenium battery technology, J. Magn. Alloys (2020).
[66] M. Mao, et al., A critical review of cathodes for rechargeable Mg batteries, Chem. Soc. Rev. 47 (23) (2018) 8804–8841.
[67] Y. Zhang, et al., Challenges and recent progress in the design of advanced electrode materials for rechargeable Mg batteries, Energy Storage Mater. 20 (2019) 118–138.
[68] K. Xu, Nonaqueous liquid electrolytes for lithium-based rechargeable batteries, Chem. Rev. 104 (10) (2004) 4303–4418.
[69] M. Asif, et al., Surface modification of tin oxide through reduced graphene oxide as a highly efficient cathode material for magnesium-ion batteries, J. Colloid Interface Sci. 561 (2020) 818–828.
[70] A. Lewandowski, A. Świderska-Mocek, Ionic liquids as electrolytes for Li-ion batteries—an overview of electrochemical studies, J. Power Sources 194 (2) (2009) 601–609.
[71] T. Maria, H. Diana, J.S.S. Thomas, Mixtures of ionic liquids as possible electrolytes for lithium ion batteries, Zeitschrift für Physikalische Chemie 226 (2) (2012) 129–139.
[72] P. Novák, J. Desilvestro, Electrochemical insertion of magnesium in metal oxides and sulfides from aprotic electrolytes, J. Electrochem. Soc. 140 (1) (1993) 140–144.
[73] P. Novák, et al., Electrochemical insertion of magnesium into hydrated vanadium bronzes, J. Electrochem. Soc. 142 (8) (1995) 2544–2550.
[74] S.H. Lee, et al., Sol gel based synthesis and electrochemistry of magnesium vanadium oxide: a promising cathode material for secondary magnesium ion batteries, ECS Electrochemistry Letters 3 (8) (2014) A87–A90.
[75] Q. An, et al., Graphene decorated vanadium oxide nanowire aerogel for long-cycle-life magnesium battery cathodes, Nano Energy 18 (2015) 265–272.
[76] K.K. Dey, et al., VO2 nanorods for efficient performance in thermal fluids and sensors, Nanoscale 7 (14) (2015) 6159–6172.
[77] C. Pei, et al., VO2 nanoflakes as the cathode material of hybrid magnesium–lithium-ion batteries with high energy density, ACS Appl. Mater. Interfaces 9 (20) (2017) 17060–17066.
[78] D. Xia, et al., Transition metal vanadates electrodes in lithium-ion batteries: a holistic review, Energy Storage Mater. (2020).
[79] H.D. Yoo, et al., High areal capacity hybrid magnesium–lithium-ion battery with 99.9% Coulombic efficiency for large-scale energy storage, ACS Appl. Mater. Interfaces 7 (12) (2015) 7001–7007.
[80] L. Li, H. Lu, K. Deng, Single CdSe nanobelts-on-electrodes Schottky junction solar cells, J. Mater. Chem. A 1 (6) (2013) 2089–2093.
[81] Y. Zhang, et al., Magnesium storage performance and mechanism of 2D-ultrathin nanosheet-assembled spinel MgIn2S4 cathode for high-temperature Mg batteries, Small 15 (36) (2019) 1902236.
[82] J.R. Nair, et al., Room temperature ionic liquid (RTIL)-based electrolyte cocktails for safe, high working potential Li-based polymer batteries, J. Power Sources 412 (2019) 398–407.
[83] Y. Li, et al., A high-voltage rechargeable magnesium-sodium hybrid battery, Nano Energy 34 (2017) 188–194.
[84] A. Byström, Otto Brotzen K.-A.W., Vanadium pentoxide: a compound with five-coordinated vanadium atoms, Acta Chem. Scand. (1950) 1119–1130.
[85] S. Yagi, et al., A concept of dual-salt polyvalent-metal storage battery, J. Mater. Chem. A 2 (4) (2014) 1144–1149.
[86] R.A. Adams, A. Varma, V.G. Pol, Temperature dependent electrochemical performance of graphite anodes for K-ion and Li-ion batteries, J. Power Sources 410-411 (2019) 124–131.
[87] B.P. Matadi, et al., Irreversible capacity loss of Li-ion batteries cycled at low temperature due to an untypical layer hindering Li diffusion into graphite electrode, J. Electrochem. Soc. 164 (12) (2017) A2374–A2389.
[88] S.S. Zhang, K. Xu, T.R. Jow, The low temperature performance of Li-ion batteries, J. Power Sources 115 (1) (2003) 137–140.
[89] G. Park, et al., The study of electrochemical properties and lithium deposition of graphite at low temperature, J. Power Sources 199 (2012) 293–299.
[90] Z. Zhang, et al., High energy density hybrid Mg2+/Li+ battery with superior ultra-low temperature performance, J. Mater. Chem. A 4 (6) (2016) 2277–2285.
[91] M. Rashad, et al., Fast kinetics of Mg2+/Li+ hybrid ions in a polyanion Li3V2(PO4)3 cathode in a wide temperature range, J. Mater. Chem. A 7 (16) (2019) 9968–9976.
[92] Y. Cheng, et al., A Bi-doped Li3V2(PO4)3/C cathode material with an enhanced high-rate capacity and long cycle stability for lithium ion batteries, Dalton Trans. 44 (40) (2015) 17579–17586.
[93] M. Rashad, et al., Simple synthesis of graphitic nanotube incorporated cobalt nanoparticles for potassium ion batteries, Ceram. Int. 46 (7) (2020) 8862–8868.
[94] X. Zhou, Y. Liu, Y. Guo, Effect of reduction agent on the performance of Li3V2(PO4)3/C positive material by one-step solid-state reaction, Electrochim. Acta 54 (8) (2009) 2253–2258.
[95] H. Yan, G. Zhang, Y. Li, Synthesis and characterization of advanced Li3V2(PO4)3 nanocrystals@conducting polymer PEDOT for high energy lithium-ion batteries, Appl. Surf. Sci. 393 (2017) 30–36.
[96] G.Q. Liu, et al., Synthesis and electrochemical properties of Li4Ti5O12, J. Alloys Compd. 509 (22) (2011) 6427–6432.
[97] W.-J. Zhang, A review of the electrochemical performance of alloy anodes for lithium-ion batteries, J. Power Sources 196 (1) (2011) 13–24.
[98] N. Wu, et al., A highly reversible, low-strain Mg-ion insertion anode material for rechargeable Mg-ion batteries, NPG Asia Mater. 6 (8) (2014) e120-e120.
[99] M. Rashad, M. Asif, Understanding the low temperature electrochemistry of magnesium-lithium hybrid ion battery in all-phenyl-complex solutions, J. Energy Chem. 56 (2021) 383–390.
[100] A.S. Keefe, et al., Temperature dependent EIS studies separating charge transfer impedance from contact impedance in lithium-ion symmetric cells, J. Electrochem. Soc. 166 (14) (2019) A3272–A3279.
[101] K.J. Laidler, The development of the Arrhenius equation, J. Chem. Educ. 61 (6) (1984) 494.
[102] Z. Liang, C. Ban, Strategies to enable reversible magnesium electrochemistry: from electrolytes to artificial solid–electrolyte interphases, Angew. Chem. Int. Ed. 60 (20) (2021) 11036–11047.
[103] K. Tang, et al., A novel regulation strategy of solid electrolyte interphase based on anion-solvent coordination for magnesium metal anode, Small 16 (49) (2020) 2005424.
[104] T. Chen, G. Sai Gautam, P. Canepa, Ionic transport in potential coating materials for Mg batteries, Chem. Mater. 31 (19) (2019) 8087–8099.
[105] J. Forero-Saboya, et al., Understanding the nature of the passivation layer enabling reversible calcium plating, Energy Environ. Sci. 13 (10) (2020) 3423–3431.
[106] K. Tang, et al., A Stable solid electrolyte interphase for magnesium metal anode evolved from a Bulky anion lithium salt, Adv. Mater. 32 (6) (2020) 1904987.
[107] X. Li, et al., Reducing Mg anode overpotential via ion conductive surface layer formation by iodine additive, Adv. Energy Mater. 8 (7) (2018) 1701728.
[108] J. Zhang, et al., Rechargeable Mg metal batteries enabled by a protection layer formed in vivo, Energy Storage Mater. 26 (2020) 408–413.
[109] S.-B. Son, et al., An artificial interphase enables reversible magnesium chemistry in carbonate electrolytes, Nat. Chem. 10 (5) (2018) 532–539.
[110] Y. Zhao, et al., A Bismuth-based protective layer for magnesium metal anode in noncorrosive electrolytes, ACS Energy Lett. (2021) 2594–2601.
[111] J. Eaves-Rathert, et al., Kinetic- versus diffusion-driven three-dimensional growth in magnesium metal battery anodes, Joule 4 (6) (2020) 1324–1336.